PROBABILISTIC ASSESSMENT OF THE CONTRIBUTION OF GEOTECHNICAL FACTORS ON OBSERVED STRUCTURAL DAMAGE IN ADAPAZARI AND DÜZCE REGIONS

A THESIS SUBMITTED TO
THE GRADUATE SCHOOL OF NATURAL AND APPLIED SCIENCES
OF
MIDDLE EAST TECHNICAL UNIVERSITY

BY

BURAK YILDIZLI

IN PARTIAL FULFILLMENT OF THE REQUIREMENTS
FOR
THE DEGREE OF MASTER OF SCIENCE
IN
CIVIL ENGINEERING

DECEMBER 2019

Approval of the thesis:

PROBABILISTIC ASSESSMENT OF THE CONTRIBUTION OF GEOTECHNICAL FACTORS ON OBSERVED STRUCTURAL DAMAGE IN ADAPAZARI AND DÜZCE REGIONS

submitted by **BURAK YILDIZLI** in partial fulfillment of the requirements for the degree of **Master of Science** i**n Civil Engineering, Middle East Technical University** by,

Prof. Dr. Halil Kalıpçılar

Dean, Graduate School of **Natural and Applied Sciences** _____

Prof. Dr. Ahmet Türer

Head of the Department, **Civil Engineering** _____

Prof. Dr. Zeynep Gülerce

Supervisor, **Civil Engineering, METU** _____

Examining Committee Members:

Prof. Dr. Erdal Çokça

Civil Engineering, METU _____

Prof. Dr. Zeynep Gülerce

Civil Engineering, METU _____

Prof. Dr. Kemal Önder Çetin

Civil Engineering, METU _____

Asst. Prof. Dr. Onur Pekcan

Civil Engineering, METU _____

Prof. Dr. Berna Unutmaz

Civil Engineering, Hacettepe University _____

Date: 06.12.2019

I hereby declare that all information in this document has been obtained and presented in accordance with academic rules and ethical conduct. I also declare that, as required by these rules and conduct, I have fully cited and referenced all material and results that are not original to this work.

Name, Last name : Burak Yıldızlı

Signature :

ABSTRACT

PROBABILISTIC ASSESSMENT OF THE CONTRIBUTION OF GEOTECHNICAL FACTORS ON OBSERVED STRUCTURAL DAMAGE IN ADAPAZARI AND DÜZCE REGIONS

Yıldızlı, Burak
Master of Science, Civil Engineering
Supervisor : Prof. Dr. Zeynep Gülerce

December 2019, 86 pages

The 1999 Kocaeli and Düzce Earthquakes caused extensive damage to the structures in Adapazarı, Düzce and surrounding cities, leading to several attempts to estimate the damage states of the existing building stock using the data collected from these destructive events. Preliminary damage state prediction models that include the geotechnical earthquake engineering factors were developed for Adapazarı after the 1999 Kocaeli earthquake; however, validation exercises were not performed using the data collected from other cities for these earthquakes. In this study, a joint database of performed subsurface soil investigations and the building stock data including the damage states and structural parameters is compiled for Adapazarı and Düzce cities and the geotechnical earthquake engineering parameters are added to the compiled database by performing site-specific ground response and seismic soil liquefaction initiation analysis. Damage state prediction models that include the number of stories, peak ground acceleration, spectral acceleration, liquefaction severity index, and liquefaction induced settlement as predictive parameters are developed by linear discriminant analysis, multinomial logistics regression, and maximum likelihood analysis methods. Models are developed for the Adapazarı dataset that includes significantly higher number of buildings and tested for the

Düzce dataset to evaluate the suitability of the selected regression approach and to analyze the contribution of ground motion and geotechnical parameters to the model performance. Analysis results showed that the number of stories is the parameter with the most significant effect on the predictive performance; while the geotechnical parameters increase the true prediction ratio in each damage state by 10%-15%. The final damage state prediction model proposed in this study estimates the damage states in Adapazarı and Düzce correctly by more than 60% for each damage state.

Keywords: 1999 Kocaeli and Düzce earthquakes, liquefaction severity index, post liquefaction volumetric settlement, site response analysis, damage state functions.

ÖZ

GEOTEKNİK DEPREM MÜHENDİSLİĞİ PARAMETRELERİNİN ADAPAZARI VE DÜZCE BÖLGELERİNDE GÖZLENEN YAPI HASARINA ETKİSİNİN OLASILIKSAL ANALİZİ

Yıldızlı, Burak
Yüksek Lisans, İnşaat Mühendisliği
Tez Yöneticisi: Prof. Dr. Zeynep Gülerce

Aralık 2019, 86 sayfa

1999 Kocaeli ve Düzce Depremleri, Adapazarı, Düzce ve çevresindeki şehirlerdeki yapılarda geniş çaplı hasara sebep olmuştur ve bu yıkıcı olaylardan toplanan veriler kullanılarak mevcut yapı stoğunun hasar durumu tahmin etmeye yönelik çeşitli çalışmalar yapılmıştır. 1999 Kocaeli Depremi'nden sonra Adapazarı'nda gözlemlenen yapısal hasarlar için, geoteknik deprem mühendisliği etkilerini de içeren hasar tahmini modelleri geliştirilmiştir ancak, önerilen modellerin bu depremler için diğer şehirlerden toplanan veriler kullanılarak doğrulama çalışmaları yapılmamıştır. Bu çalışma kapsamında, Adapazarı ve Düzce şehirleri için zemin araştırmaları, yapı stoğuna ait hasar durumları ve yapı parametrelerini içeren bir ortak veri tabanı derlenmiş, sahaya özgü zemin tepki ve sismik zemin sıvılaşma tetiklenmesi analizleri yapılarak geoteknik deprem mühendisliği parametreleri derlenen veri tabanına eklenmiştir. Tahmin parametreleri olarak, kat adedi, maksimum yer ivmesi, spektral ivme, sıvılaşma şiddet indeksi ve sıvılaşma kaynaklı oturmayı içeren hasar durumu tahmin modelleri, doğrusal diskriminant analizi, çok terimli lojistik regresyon ve maksimum olabilirlik analizi yöntemleri ile geliştirilmiştir. Modeller daha fazla sayıda yapı içeren Adapazarı veri seti için

geliştirilmiş ancak seçilen regresyon yönteminin uygunluğunu değerlendirmek ve yer hareketi ile geoteknik parametrelerin model performansına katkısını analiz etmek için Düzce veri seti ile test edilmiştir. Analiz sonuçları, kat adedinin tahmin performansı üzerinde en önemli etkiye sahip parametre olduğunu göstermiştir; geoteknik parametreler ise, hasar durumunun gerçek tahmin oranını %10-%15 oranında artırmaktadır. Bu çalışmada önerilen hasar durumu tahmin modeli, Adapazarı ve Düzce'deki hasar durumlarını herbir hasar durumu için %60'tan yüksek bir oranda doğru tahmin etmektedir.

Anahtar Kelimeler: 1999 Kocaeli ve Düzce depremleri, sıvılaşma şiddeti indeksi, sıvılaşma sonrası hacimsel oturma, saha tepki analizi, hasar durumu fonksiyonları.

ACKNOWLEDGMENTS

I would like to to express my sincere gratitude to my supervisor Prof. Dr. Zeynep Gülerce for her patience, support, advice, criticism and encouragements throughout this research. This work could not be completed without her strong support, immense patience and supportive criticism

I would like to acknowledge support from my father, late mother and my wife whose support has been helping me overcome difficulties in this very dynamic world.

TABLE OF CONTENTS

ABSTRACT v

ÖZ vii

ACKNOWLEDGMENTS ix

TABLE OF CONTENTS x

LIST OF TABLES xii

LIST OF FIGURES xiv

1 INTRODUCTION TO STRUCTURAL DAMAGE PREDICTION MODELS BASED ON EARTHQUAKE ENGINEERING PRACTICES 1

1.1 Previous Studies on Damage Prediction Modeling in Turkey 2

1.2 Previous Literature on the Relation of Structural Damage and Geotechnical Factors 17

1.3 Research Statement 21

1.4 Scope of Thesis 23

2 ADAPAZARI AND DÜZCE DATASETS COMPILED AFTER THE 1999 KOCAELI AND DÜZCE EARTHQUAKES 25

2.1 1-D Site Response Analysis and the Ground Motion Parameters Added to the Datasets 27

2.2 Parameters that are related to Soil Liquefaction 31

3 DEVELOPMENT OF DAMAGE PREDICTION MODELS BASED ON GROUND MOTION AND GEOTECHNICAL PARAMETERS 45

3.1 Linear Discriminant Analysis Method 45

3.2 Trial 1: Comparison of Tripartite and Bipartite Damage Categories 46

3.3 Trial 2: Individual Contributions of Dependent Parameters 49

3.4 Contribution of Earthquake Parameters 51
3.5 Contribution of Liquefaction Parameters 53
3.6 Trial 3: Prediction Models with Exponential Parameters 54
3.7 Multinomial Logistics Regression 56
3.8 Maximum Likelihood Regression 58
4 CONCLUSION 63
REFERENCES 65
A. Adapazarı Database Borehole Results 73
B. Düzce Database Borehole Results 80

LIST OF TABLES

TABLES

Table 1.1. Performance of the damage prediction of models developed by Yilmaz (2004) 5
Table 1.2. Percentage of true predictions for models developed by Yücemen et al. (2004) 7
Table 1.3. Estimated number of damaged buildings in Istanbul for a M_w=7.5 earthquake scenario by Strasser et al. (2008) 11
Table 1.4. Discriminant analyses results for 1992 Erzincan, 1995 Düzce and 1999 Düzce earthquake databases by Askan and Yücemen (2010) 13
Table 1.5. Observed and estimated damage from discriminant modeling for 1999 Düzce earthquake by Askan and Yücemen (2010) 14
Table 1.6. Observed and estimated damage by Ugurhan et al. (2011) 15
Table 1.7. Estimated damage for M_w=7.5 scenario by Ugurhan et al. (2011) 16
Table 2.1. Information on building stock in Adapazarı database (damage states are related to the 1999 Kocaeli Earthquake) 26
Table 2.2. Information on building stock in Düzce database (damage states are related to the 1999 Düzce Earthquake) 27
Table 2.3. Liquefaction Severity Index Classification by Yilmaz (2004) 36
Table 3.1. Coefficients of Equation 3.1 obtained by LDA and the CVs separating tripartite damage states using Adapazarı and Düzce datasets 47
Table 3.2. Coefficients of Equation 3.2 obtained by LDA and the CVs separating bipartite damage states using Adapazarı and Düzce datasets 48
Table 3.3. Discriminant coefficients for model with single parameter of number of storey (Equation 3.3) 50
Table 3.4. Discriminant coefficients for earthquake parameters and number of storey (Equation 3.4) 52

Table 3.5. Discriminant coefficients for liquefaction parameters and number of storey (Equation 3.5)..... 53
Table 3.6. Discriminant coefficients for Equation 3.6..... 55
Table 3.7. Discriminant coefficients for Equation 3.6 using combined database... 56
Table 3.8. Multinomial regression coefficients for Equation 3.7 and 3.8 57

LIST OF FIGURES

FIGURES

Figure 1.1. Wall Index and Column Index for damaged buildings in Erzincan after the 1992 earthquake (after Hassan and Sözen, 1997) 3
Figure 1.2. Spatial distribution of buildings in high risk seismic group (after Yakut et al., 2006) 9
Figure 1.3. Damage probability matrix for 1st seismic zone of Turkey for buildings deisgned according to earthquake code (AC) and not according to code (NAC) by Askan and Yücemen (2010) 12
Figure 1.4. Fragility curve for Düzce city, based on 1999 Düzce Earthquake database by Askan and Yücemen (2010) 13
Figure 1.5. Fragility curve for a low rise RC frame building proposed by Ugurhan et al. (2011) 15
Figure 1.6. Fragility curve for 3-storey poor quality irregular masonry building proposed by Ugurhan et al. (2011) 15
Figure 1.7. Observed (a) and estimated (b) Mean Damage Ratio (MDR) of 1992 Erzincan earthquake by Karimzadeh et al. (2018) 17
Figure 1.8. Estimated Mean Damage Ratio (MDR) for a M_w=7.0 event in Erzincan by Karimzadeh et al. (2018) 17
Figure 1.9. Number of observations for each integer value of LPI by Toprak and Holzer (2003) 19
Figure 1.10. Probability of liquefaction vs LPI by Toprak and Holzer (2003) 20
Figure 1.11. Centrifuge testing model by Dashti et al (2009) 21
Figure 2.1. Adapazarı database: (a) geotechnical borehole locations (in red) and (b) building stock in central municipality neighborhoods of Adapazarı 26
Figure 2.2. Düzce city map and location of investigated boreholes in the Düzce database 27
Figure 2.3. 1-D soil column used in site response analysis by Yilmaz (2004) with a sample borehole used to define the top soil layers in Adapazarı 29

Figure 2.4. 1-D soil column used in this study (with a sample borehole used to define the top soil layers) for site response analysis of Düzce borehole locations. 30
Figure 2.5. (a) Median predictions of NGAWEST-2 GMMs for Düzce city (b) 2014 WEST-2 GMPE for Adapazarı city (c) Spectral Acceleration (SA) of Sakarya and Mudurnu records (d) Surface response along with input ground motion 33
Figure 2.6. Contours for (a) PGA (g) and (b) Spectral Acceleration (g) for T=0.3s in Adapazarı (taken from Yılmaz, 2004). 34
Figure 2.7. Contours for (a) PGA (g) and (b) Spectral Acceleration (g) for T=0.3s in Düzce 35
Figure 2.8. Residual LSI values comparing updated LSI values in this study and by Yilmaz (2004) for the Adapazarı dataset. 37
Figure 2.9. Liquefaction Severity Index contours in Adapazarı (a) and in Düzce (b). 38
Figure 2.10. $N_{1,60,CS}$ correction parameter vs Fines Content (CEA2018) 40
Figure 2.11. Residual Settlement (cm) comparing updated results of this study and Yilmaz (2004) 42
Figure 2.12. Liquefaction Induced Settlement Contours in Adapazarı (a) and in Düzce (b) 44
Figure 3.1. True prediction ratios of linear discriminant and tripartite category model (Equation 3.1) 48
Figure 3.2. True prediction ratios of linear discriminant and bipartite category model derived from Adapazarı origin database (Equation 3.2) 49
Figure 3.3. True prediction ratios of linear discriminant and bipartite damage category model derived from Düzce origin database (Equation 3.2) 49
Figure 3.4. True prediction ratios of linear discriminant models using only number of storey as parameter (Equation 3.3) 51
Figure 3.5. True prediction ratios of prediction model derived from Adapazarı database (Equation 3.4) 52
Figure 3.6. True prediction ratios of prediction model derived from Düzce database (Equation 3.4) 52

Figure 3.7. True prediction ratios of prediction model derived from Adapazarı database (Equation 3.5) 54
Figure 3.8. True prediction ratios of prediction model derived from Düzce database (Equation 3.5) 54
Figure 3.9. True prediction ratios of prediction model derived from Adapazarı database (Equation 3.6) 55
Figure 3.10. True prediction ratios of prediction model derived from Düzce database (Equation 3.6) 55
Figure 3.11. True prediction ratios of prediction model derived from Adapazarı + Düzce combined database (Equation 3.6) 56
Figure 3.12. True prediction ratios of logistics regression model derived from Adapazarı origin database (Equation 3.7) 57
Figure 3.13. True prediction ratios of logistics regression model derived from Düzce origin database (Equation 3.7) 58
Figure 3.14. True prediction ratios of logistics regression model derived from Adapazarı origin database (Equation 3.9) 59
Figure 3.15. True prediction ratios of logistics regression model derived from Düzce origin database (Equation 3.9) 60
Figure 3.16. True prediction ratios of logistics regression model derived from Adapazarı origin database (Equation 3.10) 61
Figure 3.17. True prediction ratios of logistics regression model derived from Düzce origin database (Equation 3.10) 61

CHAPTER 1

INTRODUCTION TO STRUCTURAL DAMAGE PREDICTION MODELS BASED ON EARTHQUAKE ENGINEERING PRACTICES

As all other contemporary civilizations of Anatolia, Turkey has a history of damaging experiences with large magnitude earthquakes. North Anatolian Fault Zone (NAFZ) is one of the major sources of these large magnitude earthquakes; 1999 Kocaeli (M_w=7.4) and Düzce (M_w=7.2) earthquakes are the most recent examples of damaging earthquakes on this fault zone. As industrial regions neighboring to the colossal city of Istanbul; Kocaeli and Sakarya provinces had experienced not only tremendous losses of life, but also heavy damages to residential structures and industrial facilities in 1999 Kocaeli earthquake. Only three months after the Kocaeli earthquake, this region was struck again by a second earthquake on November 12, 1999, the M_w=7.2 Düzce Earthquake, which occurred roughly 100 km eastward of the first event. Having the city center located only a few kilometers away from the epicenter; the city of Düzce suffered loss of life and destruction of infrastructure, most of which were already damaged by the previous earthquake. In both of these events, geotechnical hazards like lateral spreading, sand boils and bearing capacity loss were observed and soil liquefaction was remarked to be a major contributor of damage to structures (e.g. Çetin et al. (2002), Kanıbir et al. (2006) and Aydan et al. (2004)).

Disaster and Emergency Management Presidency (AFAD), formerly known as the General Directorate of Disaster Affairs (GDDA), had compiled a comprehensive earthquake engineering database after the 1999 earthquakes. Compiled database includes various characteristics and damage states of the existing building stock in

Adapazarı and Düzce cities, in addition to the borehole logs of closely spaced geotechnical boreholes drilled in the city centers after the earthquakes. AFAD's database leaded to various studies that assess the relationship between structural engineering parameters and damage distribution; a brief summary of these studies are provided in this chapter. On the other hand, the relationship between the geotechnical engineering parameters and the structural damage that was observed after these earthquakes may be evaluated and damage prediction models based on geotechnical earthquake engineering parameters may be suggested using this database. For this purpose, previous literature on damage prediction models specific to these earthquakes are reviewed and presented in Section 1.1 to evaluate the possible existing gaps in the dataset and the statistical techniques applied for this particular problem. Only a few examples of damage prediction models based on geotechnical earthquake engineering parameters are available in the literature: these studies are summarized in Section 1.2 to discuss which geotechnical engineering parameters were used in damage prediction models.

1.1 Previous Studies on Damage Prediction Modeling in Turkey

One of the pioneering works in Turkey on damage prediction modeling was performed by Hassan and Sözen (1997) after the 1992 Erzincan earthquake (M_w=6.7). In their study, Hassan and Sözen (1997) presented a simplified method for ranking the reinforced concrete low rise buildings, depending on their vulnerability to seismic damage. Damage levels for buildings were predicted only by considering the dimensions of the structure in terms of two indices, the Column Index (CI) and the Wall Index (WI) as shown in Eq. 1.1 and 1.2:

$$WI = \frac{A_{wt}}{A_{ft}} \times 100 \tag{1.1}$$

$$CI = \frac{A_{ce}}{A_{ft}} \times 100 \tag{1.2}$$

where WI is ratio of total cross sectional area (A_{wt}) of reinforced concrete walls and 10% the masonry filler walls over the total floor area (A_{ft}), CI is 50% of the total cross sectional area of columns over the total floor area(A_{ft}). Sum of these two indices result in the Priority index (PI), which is the resultant estimator for damage:

$$PI = WI + CI \tag{1.3}$$

Proposed model was tested with the damage information in the database compiled by the reconnaissance teams from Middle East Technical University after the 1992 Erzincan earthquake. Hassan and Sözen (1997) proposed two boundaries for PI as 0.25 and 0.50 for categorizing the critical levels of the expected damage. Figure 1.1 shows the plot of CI and WI for the database compiled after 1992 Erzincan earthquake: for buildings with the lowest PI values, immediate action was suggested.

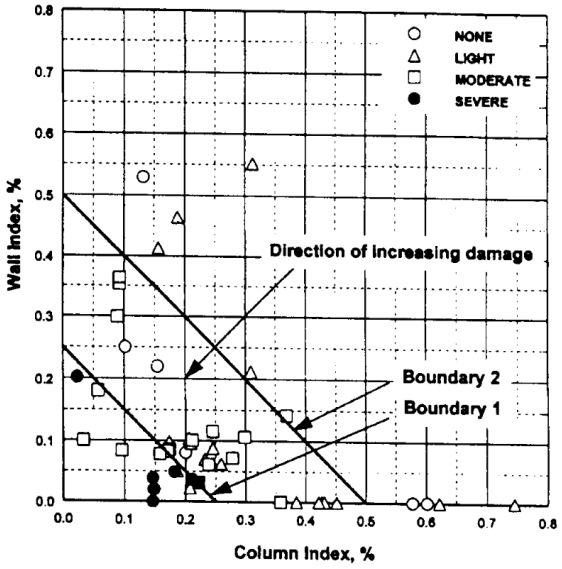

Figure 1.1. Wall Index and Column Index for damaged buildings in Erzincan after the 1992 earthquake (after Hassan and Sözen, 1997)

Yılmaz and Çetin (2003) and Yilmaz (2004) had evaluated the geotechnical and structural damage database compiled by AFAD for city of Adapazarı after the 1999 Kocaeli earthquake. One dimensional soil columns were modeled from each borehole and the results of the site-specific 1-D ground response analysis for each

borehole location were added to the database. Additionally, Yilmaz (2004) carried out seismic soil liquefaction assessment for each borehole and created hazard maps for two parameters related to soil liquefaction: the liquefaction severity index (LSI) and liquefaction induced settlements for Adapazarı city using geographic information systems (GIS). Considering both structural and geotechnical engineering parameters, the LSI, post-liquefaction settlements (S), peak ground acceleration (PGA) and spectral acceleration (Sa) at different spectral periods were selected as the contributing factors to the resulting damage states of the structures. Probabilistic models for the estimation of the damage states were developed using maximum likelihood regression methodology. Models provided by Yilmaz (2004) are given in Equations 1.4, 1.5 and 1.6, where g is the damage state indicator.

$$g = 10.65\,\exp(\mathrm{N})^{0.01} + 1.09\,PGA - 11.23 \tag{1.4}$$

$$g = 8.05\,\exp(\mathrm{N})^{0.01} + 1.06\,PGA - 0.05\,SA - 0.01\,LSI - 8.88 \tag{1.5}$$

$$g = 8.47\,\exp(\mathrm{N})^{0.01} - 0.09\,PGA + 1.11\,SA + 0.01\,LSI - 0.3\,S + 2.56 - 11.51 \tag{1.6}$$

Two damage states were defined by grouping the buildings with no damage to slight damage as non-damaged (1) and moderate to heavy damaged buildings as damaged (2). Percentages of true predictions for State (1) and State (2) for each model are given in Table 1.1: approximately 60-65% of all buildings are classified correctly using proposed models. The Adapazarı database used by Yilmaz (2004) is also utilized in this study after updating the liquefaction-related parameters; therefore, detailed descriptions of this database and discussions of Yilmaz (2004) models are given in Chapter 2.

Table 1.1. Performance of the damage prediction of models developed by Yilmaz (2004)

Model	Damaged Buildings – State (2) % True Prediction	Non Damaged Buildings - State (1) % True Prediction
Equation 1.4	62.21	64.00
Equation 1.5	61.78	65.55
Equation 1.6	60.93	65.72

The building damage database compiled by AFAD for Düzce City after the 1999 Düzce earthquake was utilized to develop damage prediction models by Yücemen et al. (2004). Compiled database includes a variety of structural parameters such as; number of stories above the ground level (N), soft story index (SSI), overhang ratio (OHR), minimum normalized lateral stiffness index (MNLSTFI), minimum normalized lateral strength index (MNLSI), and normalized redundancy score (NRS) for a total number of 484 structures. Damage states for these 484 structures were grouped into “None”, “Light”, “Moderate”, “Severe” and “Collapse” according to the level of damage in AFAD’s database. Six structural parameters given above were considered as the independent variables and the damage-predicting discriminant functions were developed using these independent variables. A stepwise procedure, comparing the discrimination significance of six input parameters had suggested that three parameters (MNLSI, OHR and MNLSTFI) do not have a significant contribution to the prediction model; therefore, Yücemen et al. (2004) re-estimated the discriminant functions with remaining parameters (N, SSI and NRS).

Damage states of the structures were considered by using two different sets for modeling the discriminant function. In the first set, damage states were simplified into tripartite subsets; None + Light damage state, Moderate damage state, and Severe + Collapse damage state. In the second set, damage states were simplified into bipartite subsets; None + Light + Moderate damage state, and Severe + Collapse

damage state, similar to the classification used by Yilmaz (2004). Discriminant scores were used to predict the damage state of buildings based on continuous parameters. It should be underlined that the selected cut-off values for separating resulting discriminant scores were not independent of the earthquake magnitude. The authors had provided the cut-off values for M_w=7.2 1999 Düzce Earthquake because of the database used in the analyses.

In conclusion, Yücemen et al. (2004) developed four damage prediction models for six or three input parameters and for bipartite or tripartite category damage states. For six structural input parameters, Equation 1.7 shows the model for bipartite damage categories; while Equation 1.8 shows the proposed model for the same damage categories after removing less significant input parameters. Six input parameter bipartite damage model had 69% true damage predictions for the initial database; whereas, three input parameter bipartite damage model had slightly improved true damage predictions (Table 1.2). In Equations 1.9 and 1.10, two more damage prediction models proposed by Yücemen et al (2004) are given for six and three structural input parameters for tripartite damage categories. Six input parameter tripartite damage model had 54.1% true damage predictions for the initial database, whereas three input parameter, tripartite damage model had 53.9% true damage predictions.

$$DI_S = 0.563n + 0.443ssi + 0.201ohr - 0.082mnlstfi - 0.161mnlsi - 0.502nrs \quad (1.7)$$

$$DI_S = 0.653n + 0.425ssi - 0.552nrs \quad (1.8)$$

$$Z_{1s} = 0.675n + 0.228ssi + 0.262ohr - 0.104mnlstfi - 0.126mnlsi - 0.511nrs$$

$$Z_{2s} = -0.356n + 0.945ssi - 0.189ohr + 0.065mnlstfi - 0.172mnlsi - 0.062nrs \quad (1.9)$$

$$Z_{1s} = 0.744n + 0.200ssi - 0.575nrs$$

$$Z_{1s} = -0.287n + 0.996ssi - 0.002nrs \quad (1.10)$$

Damage prediction models proposed by Yücemen et al. (2004) were developed using the Düzce city database; however, these models were also validated using a database from 1992 Erzincan earthquake and the combined database of Bolu – Düzce – Kaynaşlı cities after the 1999 Düzce Earthquake. Percentage of true predictions for each database is presented in Table 1.2.

Right after the damage prediction models proposed by Yücemen et al. (2004), Yakut et al. (2006) further improved these models according to the damage state classifications given in the Turkish Earthquake Code (2007). Damage prediction categories were modified such that, None + Light + Moderate damage categories were consolidated into "Life safety performance classification (LSPC)", whereas, None + Light damage categories were considered as "Immediate Occupation Performance Classification (IOPC)". Coefficients for discriminant functions and their resultant cut-off values were re-evaluated for LSPC and IOPC performance categories. Functions proposed by Yakut et al. (2006) are given in Eq. 1.11 and 1.12.

Table 1.2. Percentage of true predictions for models developed by Yücemen et al. (2004)

Model	1999 Düzce Database True Prediction	1992 Erzincan Database True Prediction	1999 Bolu Düzce Kaynaşlı Database True Prediction
6-input parameter Bipartite output	69.0 %	95.3 %	81.6 %
3-input parameter Bipartite output	69.2 %	88.4 %	82.2 %
6-input parameter Tripartite output	54.1 %	65.1 %	66.4 %
3-input parameter Tripartite output	53.9 %	62.7 %	67.1 %

$$DI_{LS} = 0.620n - 0.246mnlstfi - 0.182mnlsi - 0.699nrs + 3.269ssi + 2.728or - 4.905 \quad (1.11)$$

$$DI_{IO} = 0.808n - 0.334mnlstfi - 0.107mnlsi - 0.687nrs + 0.508ssi + 3.884or - 2.868 \quad (1.12)$$

More cut-off values for the discriminant function were proposed to extend the damage prediction models to other regions for earthquakes with different magnitudes, structures overlying various types of soil and for different distances to earthquake source. Additionally, damage prediction models were applied to Zeytinburnu municipality of Istanbul. Structural and geotechnical parameters for 16030 buildings in Zeytinburnu were compiled by METU-EERC team for developing 2003 Istanbul earthquake master plan of Istanbul Metropolitan Municipality. Discriminant scores were computed for each structure for a M_w=7.5 earthquake scenario that will occur on NAFZ at a distance roughly 10-15 km from Zeytinburnu district. Eventually, the buildings were classified under High, Medium, and Low risk categories depending on their performance for LSPC or IOPC damage levels (Figure 1.2). It was predicted that 69% of the buildings in Zeytinburnu were in high risk group with discriminant scores higher than the LSPC cut-off and these buildings need immediate attention.

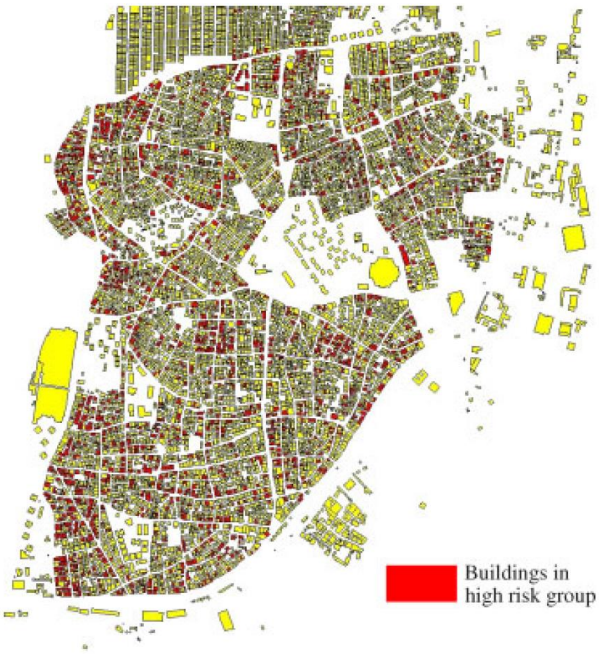

Figure 1.2. Spatial distribution of buildings in high risk seismic group (after Yakut et al., 2006)

Istanbul metropolitan city was further evaluated for an earthquake scenario of M_w=7.5 by Strasser et al. (2008) to estimate the extent of structural damage and life loss. Several intensity measures such as macro-seismic intensity, PGA and 5% damped spectral acceleration were determined for this earthquake scenario. Istanbul metropolitan city was divided into a uniform grid of 8131 cells by Strasser et al. (2008). Building database, including 562620 reinforced concrete frame structures and 173639 masonry buildings, was provided by Istanbul Metropolitan Municipality and Turkish State Statistics Institute. Building information were present for only 4014 cells out of the 8131 cells, since remaining cells were mostly not populated or low population intensity districts. Reinforced concrete buildings consist of 76.3% of all buildings, whereas masonry buildings consist of 23.5%. Buildings in the database were categorized depending on their various properties such as; being low, medium or high rise, whether it was constructed before or after the 1975 building code, steel type used in the reinforced concrete, regularity of infill walls, brick type used for load bearing walls and vault construction method for masonry structures.

Five earthquake loss estimation software; KOERILOSS, SIGE-DPC, ESCENARIS, SELENA and DBELA, were compared in terms of their estimations for structural damages and social loss. SIGE-DPC software was developed by Italian Department of Civil Protection, whereas ESCENARIS was developed by Institut Geologic de Catalunya. Both software employ the intensity parameter as the input ground motion; therefore, site-specific macroseismic intensity was computed from the relations developed by Erdik et al. (1985) and Evernden and Thompson (1985). DBELA was developed by Rose School and EUCENTRE Foundation from Pavia and this software uses response spectrum as the input ground motion intensity measure. KOERILOSS was developed by KOERI of Boğaziçi University in Istanbul. This software allows two options for input ground motion; either the earthquake intensity parameter or response spectrum is required as input. PGA was computed from the average of Boore et al. (1997), Sadigh et al. (1997), and Campbell (1997) ground motion models. Similarly, spectral accelerations were estimated by using Boore et al. (1997) and Sadigh et al. (1997) ground motion models and multiplied by site amplification factors suggested by NEHRP (1997) provisions. Software that employ the macroseismic intensity or PGA as the input had utilized the empirical mean damage ratios, empirical damage probability matrices or empirical fragility curves for damage estimation. Alternatively; software that require response spectrum as input had used the HAZUS fragility curves for estimation of damage status. DBELA software had used the vulnerability functions for damage estimation using DBELA approach of Crowley et al. (2004).

Evaluating a total of 736259 buildings in Istanbul under aforementioned software, Strasser et al. (2008) concluded that buildings with higher damages are concentrated at European side of the city, in districts of Zeytinburnu, Eminönü and Avcılar. Minimum number of expected building collapses was presented as 32148 buildings by ESCENARIS software. According to Strasser et al. (2008), expected number of collapse or beyond repair damage status estimated by each software (given in Table 1.3) shows a reasonable level of agreement with each other.

Table 1.3. Estimated number of damaged buildings in Istanbul for a M_w=7.5 earthquake scenario by Strasser et al. (2008)

Estimated Damage in EMS98 Scale	Utilized Software for Damage Estimation			
	KOERI -MSK	ESCENARIS Level 0	ESCENARIS Level 1	SIGE-DPC
Heavy (D3)	76,444	101,797	67,034	25,150 (D3+D4)
Beyond Repair (D4+D5)	40,268	53,831	32,148	1,669 (D5)
Estimated Damage in HAZUS99 Scale	Utilized Software for Damage Estimation			
	KOERI-SD		DBELA	
Moderate	195,097		200,918	
Extensive	67,395		81,497	
Collapse	34,828		46,968	

A recent study by Askan and Yücemen (2010) had discussed three different probabilistic approaches for earthquake damage estimation and compared the results. These three methods were applied for building datasets gathered after the 1992 Erzincan, 1995 Dinar and 1999 Düzce earthquakes. Resulting damage estimations were provided as the mean damage ratios for overall building databases for each city. First damage estimation method discussed by Askan and Yücemen (2010) was the damage probability matrices method (DPM). In DPM method, results were presented in a table showing resultant mean damage ratios for a range of earthquake intensity parameters. A subjective damage probability matrix was developed based on expert opinion for all four seismic regions. A second damage probability matrix of observed damage was developed from the investigations after 1992 Erzincan and 1999 Düzce earthquakes for 1st and 2nd seismic regions. Both damage matrices were blended together into a best estimate DPM with weighted averages of 25% and 75% respectively, so that a full DPM table was formed for all four seismic regions of

Turkey. An example of the final best estimate DPM for 1st seismic zone developed by Askan and Yücemen (2010) is presented in Figure 1.3.

Second damage estimation method was the reliability based damage estimation model. In this model, the exceedance probability of seismic force index over the seismic resistance index was considered. Seismic resistance index, C_R, represents the ratio of lateral seismic loading, in other words, the seismic shear force over the weight of the structure. Seismic force index, C_S, is a unitless coefficient calculated by using three inputs from Turkish Earthquake Code (2007): response spectrum, assumed damping reduction coefficient, and PGA. Probability of failure for light, moderate and severe damage status were considered as given in Equation 1.13, where the value of α is 2, 1, and 0.58 for each damage status, respectively.

Damage state (DS)	CDR (%)	MMI = V		MMI = VII		MMI = IX	
		AC	NAC	AC	NAC	AC	NAC
None	0	1	0.95	0.70	0.46	0.30	0.07
Light	5	0	0.05	0.20	0.34	0.30	0.27
Moderate	30	0	0	0.10	0.14	0.20	0.30
Heavy	70	0	0	0	0.05	0.20	0.19
Collapse	100	0	0	0	0.01	0	0.17
MDR (%)		0	0.25	4	10.4	21.5	40.7

Figure 1.3. Damage probability matrix for 1st seismic zone of Turkey for buildings deisgned according to earthquake code (AC) and not according to code (NAC) by Askan and Yücemen (2010)

$$P(failure) = P(C_R < \alpha \cdot C_S) \tag{1.13}$$

Fragility curves for reliability based damage estimation method were plotted for datasets of 1992 Erzincan, 1995 Dinar and 1999 Düzce earthquakes. In Figure 1.4, an example fragility curve derived by Askan and Yücemen (2010) from 1999 Düzce earthquake database is given for damage states of light, moderate and severe depending on earthquake intensity parameter of MMI. The third method reviewed by Askan and Yücemen (2010) was the discriminant analysis method that determines

the independent variables that are contributing significantly to the expected final damage state and develops a damage score function with discrimination limits for damage states. Seven structural parameters contributing to the final damage state; number of stories (n), normalized square root of sum of squares of inertias (SRSSI), soft story index (ss), overhang ratio index (oh), redundancy index (r), density ratio (DR) and floor regularity factor (FRF) were considered. Resultant damage indices were divided into four damage levels as none, light, moderate and severe damage states. For each city and earthquake database, individual linear damage score models were compiled. Discriminant analysis results of Askan and Yücemen (2010) are given in Table 1.4 for linear damage score functions of investigated independent variables. Developed linear discriminant models had classified the actual damage status of 1992 Erzincan, 1995 Dinar and 1999 Düzce datasets with 67.4%, 57.6% and 50.7% overall correct estimations (Table 1.5).

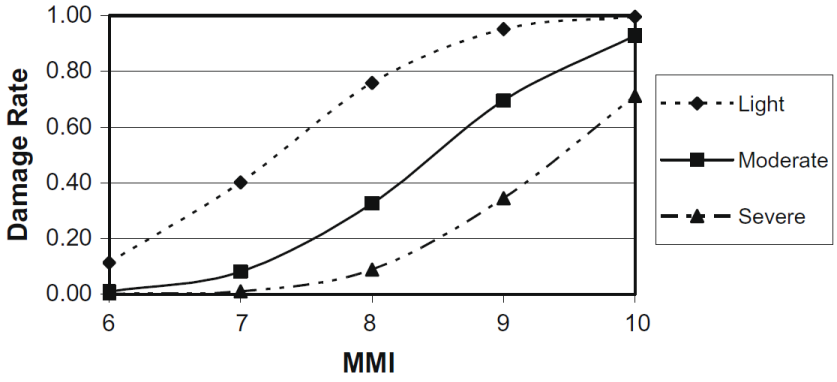

Figure 1.4. Fragility curve for Düzce city, based on 1999 Düzce Earthquake database by Askan and Yücemen (2010)

Table 1.4. Discriminant analyses results for 1992 Erzincan, 1995 Düzce and 1999 Düzce earthquake databases by Askan and Yücemen (2010)

Damage Database	n	SRSSI	r	ss	DR	oh	FRF
Düzce	-0.876	0.674	0.150	0.205	0.283	-0.409	-
Dinar	-0.062	0.187	-0.024	0.004	0.206	0.171	0.790
Erzincan	-0.187	0.036	-0.170	-0.110	0.357	0.110	0.726

Table 1.5. Observed and estimated damage from discriminant modeling for 1999 Düzce earthquake by Askan and Yücemen (2010)

Observed Damage Status	Estimated Damage Status			
	None	Light	Moderate	Severe
None	61.0 %	24.4 %	12.2 %	2.4 %
Light	14.9 %	49.3 %	13.4 %	22.4 %
Moderate	9.5 %	38.1 %	23.8 %	28.6 %
Severe	4.3 %	17.4 %	17.4 %	60.9 %

Ugurhan et al. (2011) performed a loss estimation study for Düzce, Bolu and Kaynaşlı for scenario earthquakes with varying magnitudes resulting from the Düzce segment of NAFZ. Building stock of these cities was analyzed and fragility curves were generated for masonry and reinforced concrete (R/C) structures using the methods proposed by Erberik (2008a and 2008b). Some examples of the fragility curves for masonry and R/C building are presented in Figures 1.5 and 1.6. Ground motions were simulated for earthquake scenarios with magnitudes ranging between M_w=5.5 - 7.5 by Ugurhan et al. (2011). Using PGV and PGA as the ground motion intensity measures, damage ratios were estimated from the previously generated fragility curves. For the simulations, epicenter of the scenario earthquake was assumed at the location of 1999 Düzce earthquake. Proposed method was verified by using the building datasets of Düzce, Bolu and Kaynaşlı after the 1999 Düzce earthquake, the same datasets used by Yücemen et al. (2004). Actual damage ratios were gathered from the damage observation statistics performed after 1999 Düzce earthquake; whereas, the estimated damage ratios are computed using the proposed method with fragility curves. Actual damage ratios and predicted damage ratios for Düzce, Bolu and Kaynaşlı cities are given in Table 1.6. For 1999 Düzce earthquake, proposed method predicted the damage states of three investigated cities in close compliance with actual damage states within a maximum of 6% discrepancy. Ugurhan et al. (2011) also proposed the loss estimations for these three cities for

earthquake scenarios with magnitude ranging between M_w=5.5 - 7.5. The estimated percentage of damage for the earthquake scenario with M_w=7.5 is given in Table 1.7.

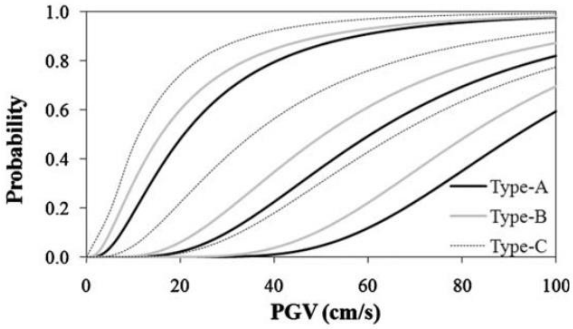

Figure 1.5. Fragility curve for a low rise RC frame building proposed by Ugurhan et al. (2011)

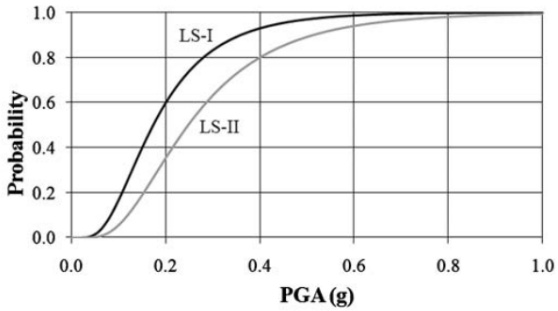

Figure 1.6. Fragility curve for 3-storey poor quality irregular masonry building proposed by Ugurhan et al. (2011)

Table 1.6. Observed and estimated damage by Ugurhan et al. (2011)

Observed Damage	Düzce City	Bolu City	Kaynaşlı City
Light	23 %	61 %	15 %
Moderate	29 %	27 %	13 %
Severe-Collapse	48 %	12 %	72 %
Estimated Damage	Düzce City	Bolu City	Kaynaşlı City
Light	24 %	66 %	12 %
Moderate	27 %	28 %	18 %
Severe-Collapse	49 %	6 %	70 %

Table 1.7. Estimated damage for M_w=7.5 scenario by Ugurhan et al. (2011)

Estimated Damage for M_w=7.5	Düzce City	Bolu City	Kaynaşlı City
Light	14 %	28 %	6 %
Moderate	19 %	31 %	9 %
Severe-Collapse	67 %	41 %	85 %

Recently, a loss estimation method was developed by Karimzadeh et al. (2018) using the data from 1992 Erzincan earthquake. Building stock of Erzincan city center had been investigated by General Statistic Agency, but further enrichment for this database was carried out by a team including Karimzadeh et al. (2018). 21 different structural models representing the local building stock were developed and used for nonlinear dynamic analysis. Ground motion simulations for scenario earthquakes with the same epicenter as 1992 Erzincan earthquake were generated and implemented in the nonlinear dynamic analysis of representative building stock models. Fragility curves were developed as a function of earthquake intensity parameters such as PGA and PGV from the results of nonlinear structural analysis. Separate fragility curves were proposed for four distinct set of damage status as none, light, moderate and severe. Erzincan city center was investigated by dividing the area into 16 central city neighborhoods. Developed fragility curves and loss estimation method was tested using earthquake intensity parameters of 1992 Erzincan earthquake. For each neighborhood, observed loss and estimated loss from the fragility models were compared. As shown in Figure 1.7, resulting damage status was consistent for 75% of the investigated neighborhoods.

Karimzadeh et al. (2018) also performed the loss estimation for an earthquake scenario of M_w=7.0 with same source and path as 1992 Erzincan earthquake, and expected damage status in Erzincan for this particular scenario is presented in Figure 1.8. Significant damages for all central city neighborhoods was estimated for this

scenario event, due to very close distance of the city center to NAFZ and high seismic vulnerability of buildings within the central city limits.

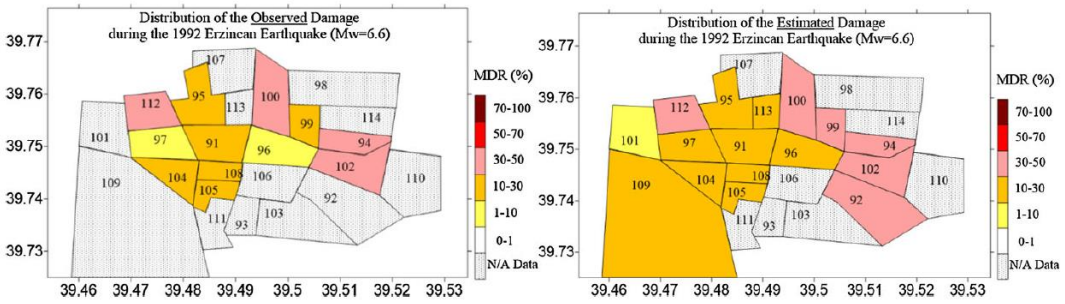

Figure 1.7. Observed (a) and estimated (b) Mean Damage Ratio (MDR) of 1992 Erzincan earthquake by Karimzadeh et al. (2018)

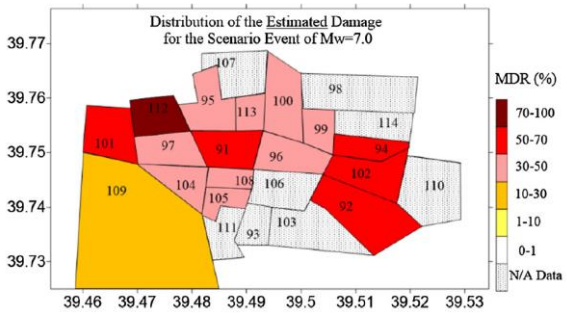

Figure 1.8. Estimated Mean Damage Ratio (MDR) for a M_w=7.0 event in Erzincan by Karimzadeh et al. (2018)

1.2 Previous Literature on the Relation of Structural Damage and Geotechnical Factors

Studies that relate the geotechnical earthquake engineering parameters with the structural damage are rather limited and available studies have generally used either liquefaction related indices or liquefaction-induced strains or settlements. In order to understand the effect of soil liquefaction on the expected structural damage, the liquefaction potential of the full (complete) soil profile should be evaluated rather than the liquefaction potential of a particular layer. Iwasaki et al. (1978) developed

a simplified method for liquefaction potential estimation using a series of indices such as; liquefaction resistance factor and liquefaction potential index. Liquefaction resistance factor is the ratio of resistance of a soil element to the dynamic loads induced by earthquake. It is denoted by F_L in Equation 1.14, where R is resistance of soil element and L is the seismic loads on a soil element.

$$F_L = \frac{R}{L} \tag{1.14}$$

Iwasaki et al. (1978) assumed that the severity of liquefaction should be directly proportional with the thickness of the liquefiable layer, distance from the liquefiable layer to surface level and the amount by which the ratio of the liquefaction resistance to the load imposed by the earthquake is less than 1. In order to reflect decreasing severity of liquefaction with increasing depth, Iwasaki et al. (1978) suggested a weighting function, w(z). Proposed weight function and liquefaction potential formula by Iwasaki et al. (1978) are given in Equations 1.15 and 1.16.

$$w(z) = 1 - 0.05z \tag{1.15}$$

$$LPI = \int_0^{20m} (1 - F_L) \cdot w(z)\, dz \tag{1.16}$$

In summary, LPI combines the depth, thickness, and liquefaction resistance factor into a single parameter, representing the full soil column. Depending on the evaluated case studies, Iwasaki et al. (1978) suggested that severe liquefaction is not expected for LPI values below 5 and severe liquefaction is expected for LPI values above 15.

USGS had compiled a database of standard penetration test (SPT) and cone penetration test (CPT) for the liquefied and non-liquefied locations following the 1989 Loma Prieta (M_w=6.9) earthquake. Toprak et al. (1999) had enriched this database with information from other earthquakes with similar moment magnitudes. Using logistics regression statistical technique, the authors developed correlation models for estimating liquefaction probability for SPT and CPT results as given in Equation 1.17 and 1.18, respectively.

$$Logit(P_L) = \ln\left[\frac{P_L}{1-P_L}\right] = 10.4459 - 0.2295\ (N_1)_{60cs} + 4.0573\ \ln(\frac{CSR}{MSF}) \qquad (1.17)$$

$$Logit(P_L) = \ln\left[\frac{P_L}{1-P_L}\right] = 11.6896 - 0.0567\ (q_{c1N})_{cs} + 4.0817\ \ln(CSR) \qquad (1.18)$$

These correlations were developed for M_W=7.5 earthquake and the application of Youd and Idriss (1997) magnitude scaling factor was suggested for adjusting the proposed models for earthquakes with other magnitudes.

A couple years later, Toprak and Holzer (2003) combined Eq. 1.18 with Eq. 1.16 to evaluate the predictive capability of LPI. They studied the USGS database of CPT soundings and calculated the LPI values for historic liquefaction sites of Monterey Bay, Imperial Valley and San Fernando Valley. At these sites, liquefaction was observed after earthquakes of 1971 San Fernando (M_w=6.6), 1979 Imperial Valley (M_w=6.5), 1987 Superstition Hills (M_w=6.6), 1989 Loma Prieta (M_w=6.9) and 1994 Northridge (M_w=6.7). Probability of liquefaction was evaluated as the percentage of liquefied sites among all the mentioned historical liquefaction sites. For each integer value of LPI, probability of liquefaction was computed as the ratio of liquefied number of observations to overall number of observations. Plot of the number of liquefied and non-liquefied observations for each LPI value is given in Figure 1.9.

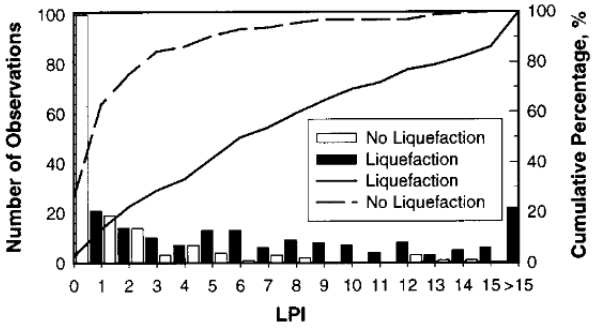

Figure 1.9. Number of observations for each integer value of LPI by Toprak and Holzer (2003)

Toprak and Holzer (2003) compared the probabilities of liquefaction which were determined from observations with the LPI values they computed from USGS

database using CPT soundings. Results are presented in Figure 1.10, where a positive relation is observed between liquefaction probability and LPI. Results of their study indicate that LPI is a useful indicator for liquefaction hazard mapping. Toprak and Holzer (2003) suggest that for LPI values of 5 and 15, probability of liquefaction is 58% and 93%, respectively. In Monterey Bay region, sand boils were observed for locations with 5 or higher LPI, and lateral spreading was observed for locations with 15 or higher LPI.

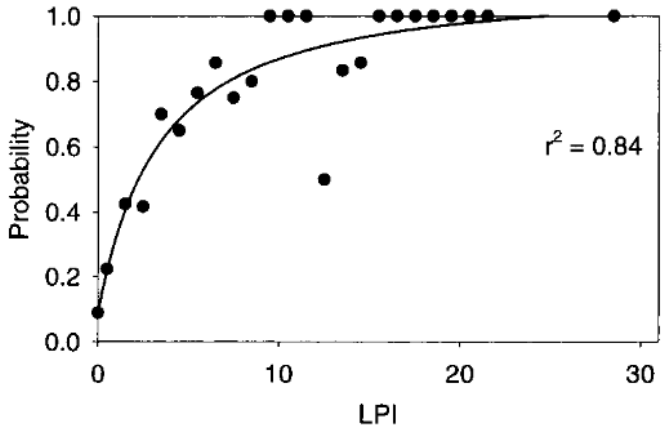

Figure 1.10. Probability of liquefaction vs LPI by Toprak and Holzer (2003)

Dashti et al. (2010) discussed the two main contributors of liquefaction-induced settlements as the modes of volumetric deformation and deviatoric deformation. During liquefaction, localized volumetric strains were observed due to partial drainage of pore water during strong shaking, although drainage is usually assumed to be nonexistent during shaking. Sedimentation settlement was reported to be caused by soil skeleton breakdown and solidification at the base of liquefied soil layer. Consolidation settlement is also triggered by net excess pore pressure dissipation caused by shaking. In addition to these volumetric strain contributing elements; following deviatoric deformations factors were underlined by Dashti et al. (2010): partial bearing capacity failure due to strength loss and soil structure interaction induced settlements during cyclic loading.

Dashti et al. (2010) carried out a number of centrifuge experiments that models the interactive behavior of liquefiable soil and buildings with shallow foundations. Structures with several different shallow foundations with different B/H ratios were modeled over dense and loose Nevada sand and Monterey sand. A recording from 1995 Kobe earthquake recorded at 83 m depth was applied as the input motion. An example centrifuge test model used by Dashti et al. (2010) is shown in Figure 1.11.

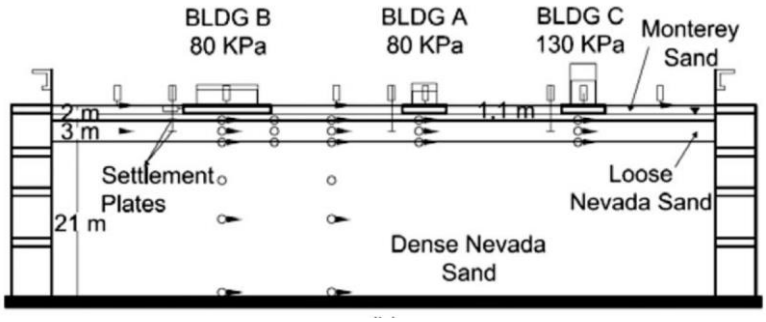

Figure 1.11. Centrifuge testing model by Dashti et al (2009)

It was understood from these tests that shallow foundations under seismic cyclic loads, settle more than the expected free-field settlements and building settlements are not proportional to the thickness of liquefiable layer. Significant excess pore pressures are reported under shallow foundations and drastically reduced strength of soil was observed during seismic loading.

1.3 Research Statement

Previous damage prediction models in the literature have generally employed the parameters related to building dimensions, material type and the design of the structural frame. Especially after the 1999 earthquakes in Turkey, several prediction models based on the structural parameters were developed and tested, specifically for Düzce, Kaynaşlı, and Erzincan showing that approximately 60-65% of the damage states may be predicted correctly using these models. Damage prediction models that include geotechnical parameters are very limited in the current literature

and non-existing for Turkey. Limited number of studies that analyzed the relation between the structural damage and geotechnical factors showed that, indices that represent the liquefaction potential of the soil profile and liquefaction-induced settlements might correlate well with the structural damage distribution. An initial attempt was made by Yilmaz and Çetin (2003) and Yilmaz (2004) to include geotechnical earthquake engineering parameters in damage prediction models using the comprehensive dataset of Adapazarı. Preliminary results of Yılmaz (2004) were promising: approximately 60-65% of the damage states in Adapazarı database were predicted correctly by the proposed model. On the other hand, the preliminary model proposed by Yılmaz (2004) had certain limitations due to the employed statistical approach and the author did not have the chance of validating the model results for other datasets such as the Düzce dataset. Additionally, studies published since 2004 underlined the controversial issues and brought in several improvements in the soil liquefaction potential assessment methods, calling for an update of the Yilmaz (2004) damage prediction model in terms of liquefaction-related parameters.

The main objectives of this study are: (i) to update the preliminary model proposed by Yilmaz (2004) in terms of liquefaction-related predictive parameters and statistical approach, and (ii) to validate the proposed model with a different dataset that have adequate information about the geotechnical factors and similar building conditions. AFAD's Düzce database collected after the 1999 Düzce earthquake is selected as the test dataset and the geotechnical boreholes in Düzce city are analyzed and integrated into this database in a consistent manner with the Adapazarı database. In the last decade, new predictive models for cyclic volumetric and deviatoric strains were proposed by Çetin et al. (2009) and the empirical models for predicting the probability of liquefaction was updated by Çetin et al. (2018). These new equations are utilized to determine the liquefaction severity index and liquefaction induced settlements for each borehole of Adapazarı and Düzce database. Additionally, 1-D site-specific ground response analyses were performed for the simplified soil models representing the boreholes in Düzce database. The damage prediction models are

developed for both datasets individually and for the combined dataset using the maximum likelihood methodology, discriminant analysis and logistic regression techniques. Model performance is evaluated by analyzing the percentage of true predictions in the host dataset and in the test dataset, indicating that the preliminary model proposed by Yılmaz (2004) is improved, especially in predicting the damaged cases.

1.4 Scope of Thesis

Following this introduction on 1999 Kocaeli and Düzce earthquakes and the summary of previous studies on damage prediction models in the literature; in Chapter 2, the Adapazarı and Düzce datasets will be presented. Because the building damage database and the 1-D site response analysis for each geotechnical borehole in Adapazarı were elaborated by Yilmaz (2004), only a brief summary of these issues are provided in Chapter 2. On the other hand, the liquefaction potential assessment is updated and the liquefaction-induced settlements are re-calculated for Adapazarı city; therefore, details of the update along with the updated hazard maps are presented in details in Chapter 2. In Chapter 2, the compilation efforts for Düzce database are also presented, following the same manner of Adapazarı database. The spatial distribution of predictive parameters such as PGA, liquefaction severity index, etc. in Düzce city is also provided in this chapter. Chapter 3 elaborates the development and testing of the damage prediction models for Düzce and Adapazarı datasets in terms of parameter significance and prediction performance. Finally in Chapter 4, main finding of this study are discussed and the preferred damage prediction model that might be applied for future damage prediction studies is selected.

CHAPTER 2

ADAPAZARI AND DÜZCE DATASETS COMPILED AFTER THE 1999 KOCAELI AND DÜZCE EARTHQUAKES

After the 1999 Kocaeli and Düzce earthquakes, General Directorate of Disaster Affairs had compiled separate datasets that contain almost the same type of information for Adapazarı and Düzce cities. The Adapazarı database includes 236 geotechnical borehole logs and various characteristics of the building stock along with their damage states. As shown in Figure 2.1(a), the spatial distribution of these boreholes (red points) covers the central neighborhoods of Adapazarı Municipality, as most of the building stock of Adapazarı was located in the regions marked with blue lines. The spatial distribution of the 17142 buildings available in the AFAD's database is shown in Figure 2.1(b) and the summary of the number of stories and damage states in the Adapazarı building dataset is provided in Table 2.1. Adapazarı city center has been growing toward west, northwest and south after the 1999 Kocaeli earthquake. Administrative buildings were moved northwest to Karaman district where new residential structures were constructed. In addition, the old city center has expanded to west and south, towards Serdivan and Arifiye districts along the two main highways to that connects the city to Istanbul. Fortunately, the spatial distribution of the geotechnical boreholes on the south of the old city center also covers the southward expansion of the new Adapazarı city.

The Düzce database includes more detailed parameters related to the building stock such as the areas of the ground and normal floors, the number and the total area of columns, and damage status after 1999 Düzce earthquake; however, the number of buildings included in the database is limited to 428. Similar to the Adapazarı database, Düzce database involves 182 geotechnical borehole logs scattered throughout the Düzce city. Locations of these boreholes (red dots) are plotted over

the layout of Düzce in Figure 2.2. It should be noted that 1- and 2-storey buildings in the Adapazarı and Düzce datasets are discarded in this study because they were not designed according to the standard engineering practice. Statistics of the remaining buildings in the Düzce database is provided in Table 2.2.

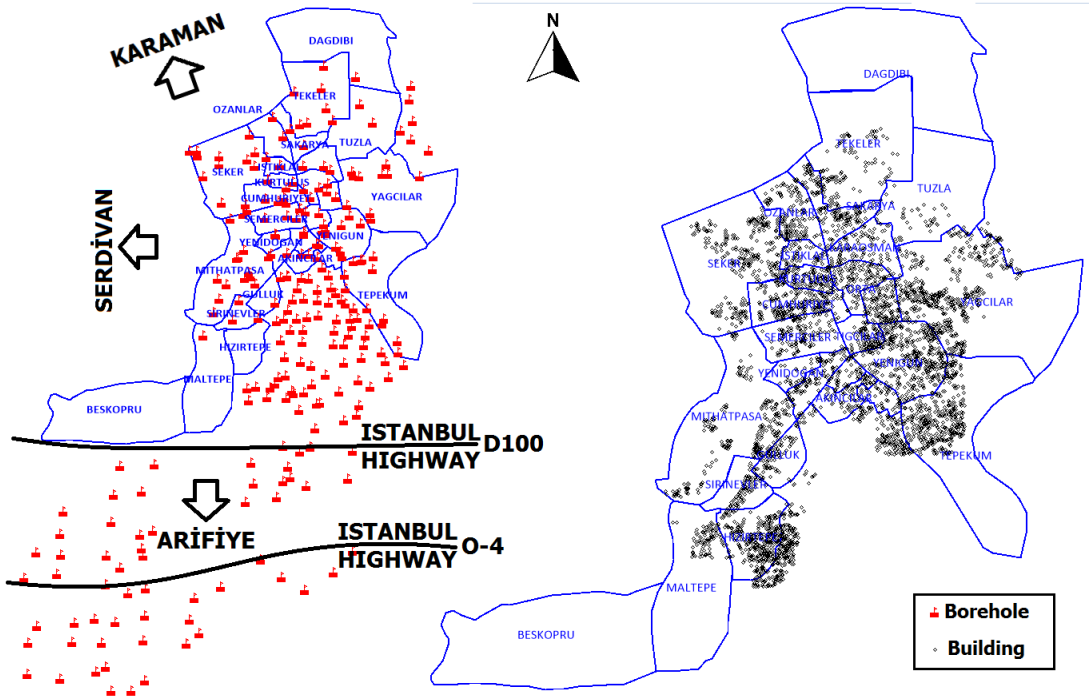

(a) (b)

Figure 2.1. Adapazarı database: (a) geotechnical borehole locations (in red) and (b) building stock in central municipality neighborhoods of Adapazarı

Table 2.1. Information on building stock in Adapazarı database (damage states are related to the 1999 Kocaeli Earthquake)

Damage State	Number of Storeys						Total
	1	2	3	4	5	>5	
No Damage: 1	8395	5012	2355	989	349	42	17142
Moderate Damage: 2	289	301	131	163	139	22	1045
Heavy Damage: 3	972	557	209	167	112	12	2029

Figure 2.2. Düzce city map and location of investigated boreholes in the Düzce database

Table 2.2. Information on building stock in Düzce database (damage states are related to the 1999 Düzce Earthquake)

Damage State	Number of Storeys					Total
	3	4	5	6	7	
No Damage: 1	81	60	48	2	1	192
Moderate Damage: 2	28	60	56	3	-	147
Heavy Damage: 3	15	23	23	4	-	65

2.1 1-D Site Response Analysis and the Ground Motion Parameters Added to the Datasets

The geotechnical boreholes drilled after both earthquakes were shallow boreholes; typically reaching down to 10-15 meters depth, but not extending to the hard and stiff layers that can be considered as the engineering bedrock. Available data from

deep boreholes are used to extend the simplified soil columns up to 150m depth in Adapazarı and 35m depth in Düzce. Deep borehole logs for Adapazarı were gathered from the soil investigations of State Hydraulic Works by Yilmaz (2004). In these deep borehole logs, an approximately 70m thick clay layer was located under the top soil layers, overlying a 15m thick gravel layer, which is followed by a second layer of 50m thick clay layer reaching down to 150m depth. Engineering bedrock was observed at approximately 150m depth in the deep borehole logs of Adapazarı. Deeper soil layers for Düzce boreholes are modelled using the shear wave velocity profile and the geotechnical report of Düzce strong ground motion station, where the engineering bedrock is located at 28-33 m depth, overlaid with a 5m thick gravel layer and 13m thick sand deposit (http://kyhdata.deprem.gov.tr, Station DUZ 8101, last accessed on December, 2019). In 1-D site response analysis, the soil layers below 15 meters is assumed to be the same for each location (as modeled using the deep boreholes); whereas the top layers (between 0-15m depth) are defined specifically for each boring log. Examples for simplified soil columns utilized in 1-D site response analysis for Adapazarı and Düzce cities are presented in Figures 2.3 and 2.4, respectively.

Measured shear wave velocity (V_s) profiles are not available for the borehole locations in Adapazarı and Düzce; therefore, V_s values are estimated from the average of the SPT (Standard Penetration Test) N-based empirical V_s relationships proposed by Ohta and Goto (1978), Seed et al (1983), Sykora and Stokoe (1983) Dickenson (1994), and Hasancebi and Ulusay (2007) for the top soil layers of the simplified soil columns. Only a limited number of laboratory test results were available for samples retrieved from the boreholes in Adapazarı; therefore, the unit weights were assigned to the soil layers based on laboratory test results when available (Yilmaz, 2004). For the cases where laboratory test results were not available, the average unit weight of the soil samples (18.5 kN/m^3) was utilized. To model the equivalent-linear soil properties, the average modulus degradation and damping curves proposed by Seed and Idriss (1970) was used for sand; whereas,

modulus degradation and damping proposed by Vucetic and Dobry (1991) with PI=15, 30 and 50 were selected for silt and clay layers. Average modulus degradation curves developed by Seed at al. (1986) Schnabel (1973) for gravel and rock were employed for gravel and weathered rock, respectively.

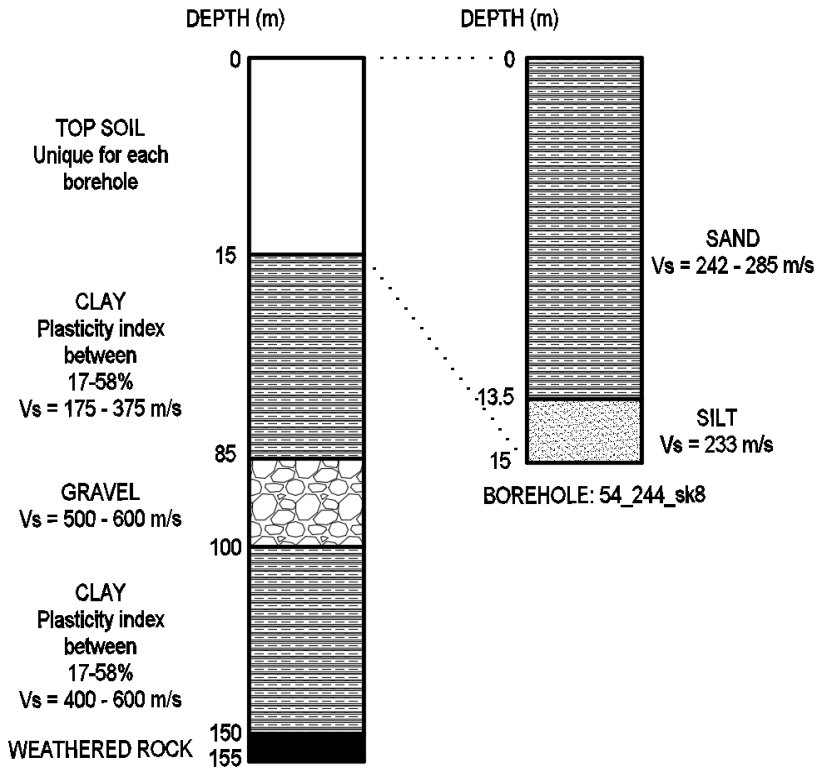

Figure 2.3. 1-D soil column used in site response analysis by Yilmaz (2004) with a sample borehole used to define the top soil layers in Adapazarı

The site response analyses for the locations of 236 boreholes in the Adapazarı dataset were conducted by Yilmaz (2004) using the SHAKE 1-D equivalent-linear site response analysis software developed by Schnabel et al. (1972). These analyses were not repeated within the contents of this study. The E-W component of the strong ground motion at Sakarya station (station code 5401) recorded during the 1999 Kocaeli earthquake was utilized in site response analysis without applying a scale factor, as this was the closest recording to the Adapazarı city at a distance of 4 km to the city center. Figure 2.5(a) shows that the average median predictions of the Next

Generation Attenuation (NGA-West 2,) ground motion models (GMMs) (Bozorgnia et al., 2014) are consistent with the input motion used in the site response analysis performed for Adapazarı dataset (Figure 2.5c).

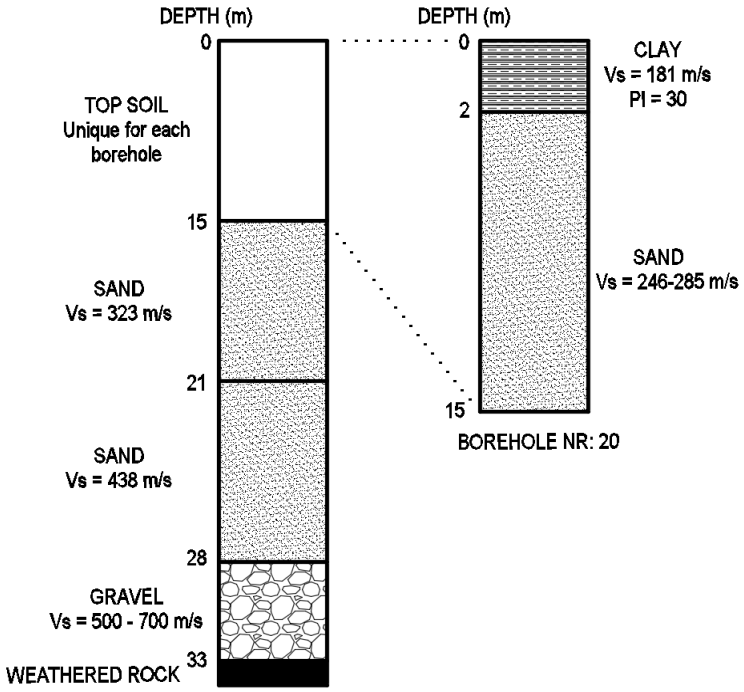

Figure 2.4. 1-D soil column used in this study (with a sample borehole used to define the top soil layers) for site response analysis of Düzce borehole locations

The 1-D equivalent-linear site response analyses for the locations of 182 boreholes in the Düzce dataset were conducted using the DEEPSOIL software (Hashash, 2012) in this study. The strong ground motion at Mudurnu station (station code 1406) recorded during the 1999 Düzce earthquake was selected as the input motion. Compared to other stations recorded this earthquake, Mudurnu station has the highest average shear wave velocity at the first 30m ($V_{s,30}$) and is located relatively closer to Düzce. On the other hand, rupture distance for Mudurnu station was 42km and the Düzce city was located only 8 km away from the fault plane; therefore, the record should be scaled before utilizing in the site response analysis. To determine the scale factor, average median predictions of the NGA-West 2 GMMs shown in Figure

2.5(b) for M_w=7.2, R_{rup}=8km and V_{S30}=760 m/s is used. The original and scaled response spectra for the input ground motions used in this study for Düzce and by Yilmaz (2004) for Adapazarı are given in Figure 2.5(c).

The response spectrum at the surface for each borehole location is estimated in site response analyses (an example is provided in Figure 2.5d) and transferred into the Adapazarı and Düzce GIS (geographic information system) dataset. The spatial variations of the site-specific peak ground accelerations (PGA) for Adapazarı and Düzce are provided in Figures 2.6(a) and 2.7(a), respectively. Additionally, site-specific spectral acceleration values at several different spectral periods were transferred to the GIS framework and the contour maps for each spectral period were prepared. The spatial distributions of spectral accelerations at T=0.3s for Adapazarı and Düzce are shown in Figures 2.6(b) and 2.7(b), respectively. Figures 2.6 and 2.7 indicate severe amplification of the input ground motion due to local soil conditions. The PGA of the input ground motion for Düzce is 0.32g; while the PGA values are amplified up to 0.64g at the city center. For these locations, significantly high spectral accelerations (reaching up to 3.06g) are observed. In Adapazarı, the site amplification factors for PGA are less prominent, due to significant de-amplification effects. Similarly, spectral accelerations at the Adapazarı city center are relatively lower (reaching up to 0.74g) when compared to the spectral accelerations in Düzce city center.

2.2 Parameters that are related to Soil Liquefaction

The geotechnical field and laboratory test results in the Adapazarı and Düzce datasets include most of the parameters required to perform seismic soil liquefaction assessment such as; fines content (FC), SPT N-value, groundwater table depth and the density of soil layers. Using the avaliable information, effective stress (σ'_v) and total stress (σ_v) of the soil layers are calculated and the SPT N-values are corrected for overburden pressure (Liao and Whitman, 1986). The shear mass participation

factor (r_d) and the in-situ cyclic stress ratio (CSR_{eq}) are required to calculate the seismic demand for seismic soil liquefaction assessment. The in-situ CSR_{eq} is calculated by using the simplified procedure proposed by Seed and Idriss (1971) and the r_d values are estimated by using the model proposed by Çetin et al. (2004) as shown in Equations 2.1 and 2.2, respectively. The site-specific PGA value at the surface of the borehole that was estimated by the 1-D site response analysis is utilized as a_{max} in Eq. 2.1. The moment magnitude, M_w, is taken as 7.4 and 7.2 for the Adapazarı and Düzce datasets, respectively.

$$CSR_{eq} = \frac{a_{\max}}{g} \cdot \frac{\sigma_v}{\sigma'_v} \cdot r_d \tag{2.1}$$

$$r_d(d, M_w, a_{\max}, V_{s,12}) = \frac{\left[1 + \frac{-23.013 - 2.949 \cdot a_{\max} + 0.999 \cdot M_w + 0.0525 \cdot V_{s,12}}{16.258 + 0.201 \cdot e^{0.341 \cdot (-d + 0.0785 \cdot V_{s,12} + 7.586)}}\right]}{\left[1 + \frac{-23.013 - 2.949 \cdot a_{\max} + 0.999 \cdot M_w + 0.0525 \cdot V_{s,12}}{16.258 + 0.201 \cdot e^{0.341 \cdot (0.0785 \cdot V_{s,12} + 7.586)}}\right]} \pm \sigma_{\varepsilon r_d} \tag{2.2}$$

Probability of liquefaction initiation of a soil layer was calculated by the model proposed by Çetin et al. (2004) (Equation 2.3) for the Adapazarı dataset by Yilmaz (2004). In Equation 2.3, the liquefaction initiation potential (P_L) is given as the function of CSR_{eq}, overburden corrected SPT blow counts ($N_{1,60}$), FC, σ'_v, and M_w. Recently, the model proposed by Çetin et al. (2004) was updated by Çetin et al. (2018) (hereafter CEA2018). For the CEA2018 model, the case studies in the original model's database were reviewed and new cases were added from studies of Idriss and Boulanger (2010) and Boulanger and Idriss (2014). Typological errors in the previous mathematical model and atmospheric pressure conversion constants were corrected and the unit weights and water content of soil layers were updated based on the SPT-N values. Functional form of the new CEA2018 model is the same as the old version, but the model coefficients were re-estimated as shown in Equation 2.4. In this study, the probability of liquefaction value for the boreholes in the

Adapazarı dataset are updated and the probability of liquefaction values for the boreholes in the Düzce dataset are estimated in compliance with the updated CEA2018 model.

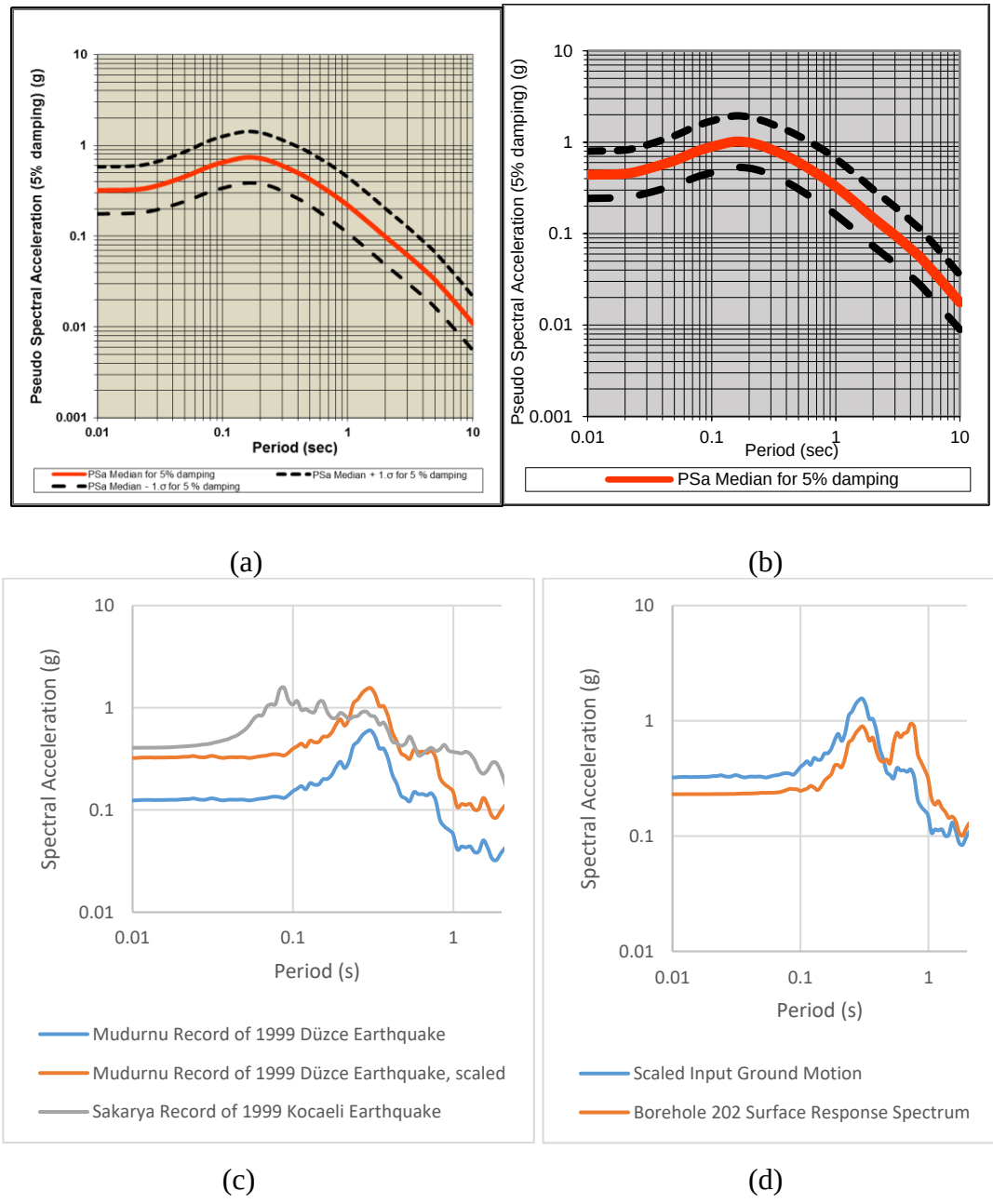

Figure 2.5. (a) Median predictions of NGAWEST-2 GMMs for Düzce city (b) 2014 WEST-2 GMPE for Adapazarı city (c) Spectral Acceleration (SA) of Sakarya and Mudurnu records (d) Surface response along with input ground motion

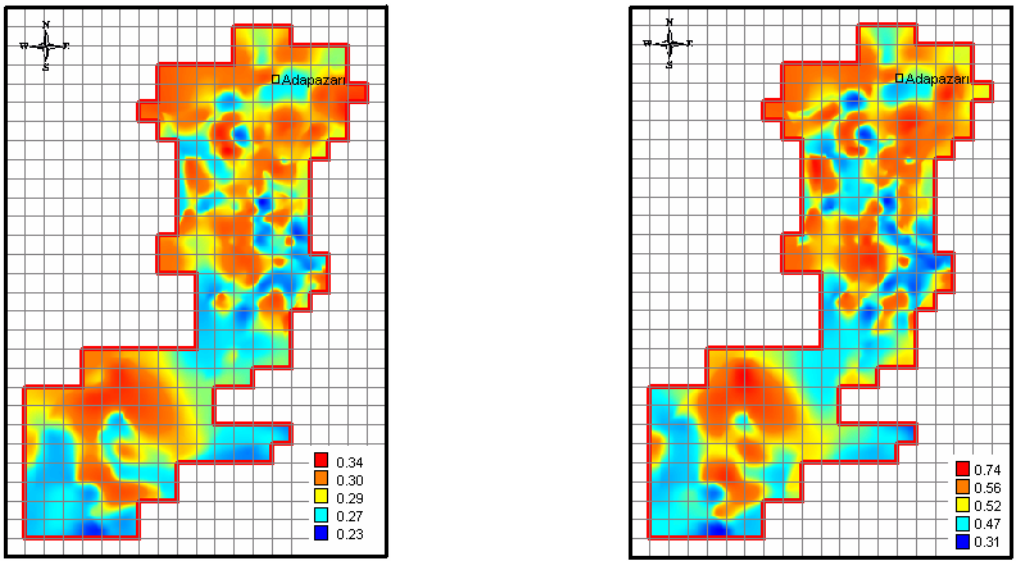

(a) (b)

Figure 2.6. Contours for (a) PGA (g) and (b) Spectral Acceleration (g) for T=0.3s in Adapazarı (taken from Yılmaz, 2004).

$$P_L = \Phi\left(-\frac{\left(\begin{array}{l} N_{1,60}\cdot(1+0.004\cdot FC)-13.32\cdot\ln(CSR)- \\ 29.53\cdot\ln(M_w)-3.70\cdot\ln(\sigma_v')+0.05\cdot FC+44.97 \end{array}\right)}{2.70}\right) \tag{2.3}$$

$$P_L = \Phi\left(-\frac{\left(\begin{array}{l} N_{1,60}\cdot(1+0.00167\cdot FC)-11.771\cdot\ln\left(CSR_{\sigma_v',\alpha=0,M_W}\right) \\ -27.352\cdot\ln(M_w)-3.958\cdot\ln\left(\frac{\sigma_v'}{P_a}\right)+0.089\cdot FC+16.084 \end{array}\right)}{2.95}\right) \tag{2.4}$$

Inspired by Liquefaction Potential Index from methodology proposed by Iwasaki et al. (1982), Yilmaz and Çetin (2003) developed the Liquefaction Severity Index (LSI) as a parameter to estimate the potential of failure of soil column rather than potential failure of a single soil layer as shown in Equation 2.5.

$$LSI = \int_0^{20} PL \cdot TH \cdot WF \; dz \tag{2.5}$$

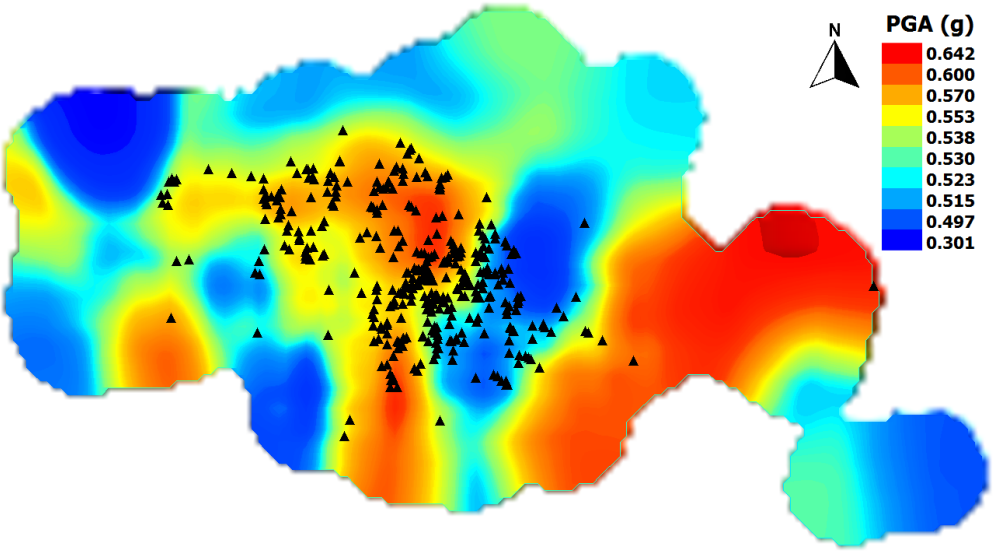

(a)

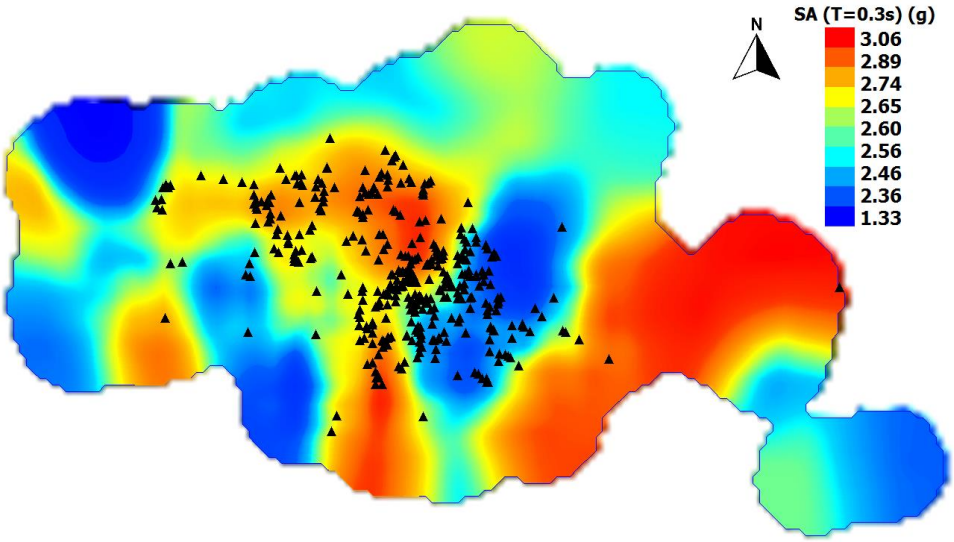

(b)

Figure 2.7. Contours for (a) PGA (g) and (b) Spectral Acceleration (g) for T=0.3s in Düzce

In Equation 2.5, PL is the average probability of liquefaction for the soil layer, TH is the thickness of the potentially liquefiable layer and WF is a weight factor decreasing with depth, expressed in terms of depth (z) in the following equation:

$$WF(z) = 1 - 0.05\,z \tag{2.6}$$

Yılmaz (2004) computed the LSI for each borehole in the Adapazarı dataset and transferred the results to the GIS framework. Based on the relationship between the spatial distribution of the damaged buildings and the contours of LSI, boundaries given in Table 2.3 were recommended by Yılmaz (2004).

Table 2.3. Liquefaction Severity Index Classification by Yilmaz (2004)

Liquefaction Severity Index	Liquefaction Failure Potential
0 >LSI > 0.35	Extremely Low
0.35 >LSI > 1.30	Low
1.30 >LSI > 2.5	High
2.5 > LSI = 10.0	Extremely High

Becouse the probability of liquefaction values at every SPT test level in the boreholes located in Adapazarı dataset is updated based on CEA2018 model; the LSI values for the Adapazarı boreholes are re-calculated. Residual LSI value for each borehole was calculated by the subtracting the updated LSI value from the LSI value given by Yılmaz (2004) and the distribution of the residuals are plotted in Figure 2.8. According to Figure 2.8, updating the probability of liquefaction and the LSI resulted in less than ±0.5 change in LSI for 229 of the boreholes. Only for 17 boreholes, the LSI values increased significantly; whereas, a significant decrease in LSI was observed in 4 boreholes. The LSI values are calculated for the boreholes in the Düzce dataset using the same methodology described for the Adapazarı boreholes. The LSI values are transefferd to the GIS framework and the raster images are drawn using the inverse distance weighting method. Resulting contour maps are given in

Figures 2.9 (a) and (b) along with central neighborhoods of Adapazarı and locations of buildings of Düzce within the dataset. Becouse the site-specific PGA values in Düzce city are significantly higher than the site-specific PGA values in Adapazarı, the LSI values in Düzce are also higher than the LSI values in Adapazarı. It should be underlined that the majority of the buildings located in the Düzce dataset are underlain by high LSI values.

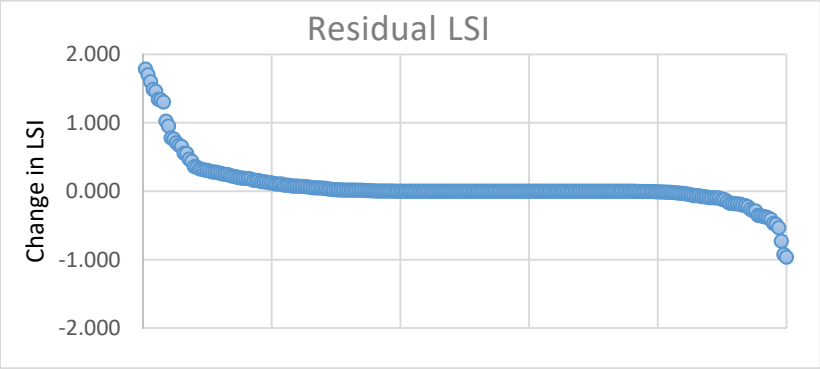

Figure 2.8. Residual LSI values comparing updated LSI values in this study and by Yilmaz (2004) for the Adapazarı dataset.

Liquefaction triggers volumetric and deviatoric strains in sandy soils because of the excess pore pressures generated during seismic ground motions. Volumetric and deviatoric straining cause foundation deformations, thus resulting in damage to structures. In the work of Yilmaz (2004), methodology in Equation 2.7 and 2.8 was employed in order to estimate the liquefaction induced volumetric and deviatoric settlement. This method expresses volumetric and deviatoric straining as a function of field cyclic stress ratio (CSR_{eq}), overburden corrected SPT blow counts ($N_{1,60}$), fines content (FC), effective stress (σ'_v), fines content(FC) and moment magnitude of the earthquake (M_w).

$$\gamma = \frac{-N_{1,60}\,(1+0.001\,FC)+29.2231\ln(M_w)+3.6604\ln\sigma'_v-0.05\,FC}{0.0508\,N_{1,60}+0.1853} \quad (2.7)$$

$$\varepsilon_v = \frac{-N_{1,60}\,(1+FC)+152.0203\ln(M_w)+467.0402\ln\sigma'_v-0.05\,FC}{104.2823\,N_{1,60}+464.1991} \quad (2.8)$$

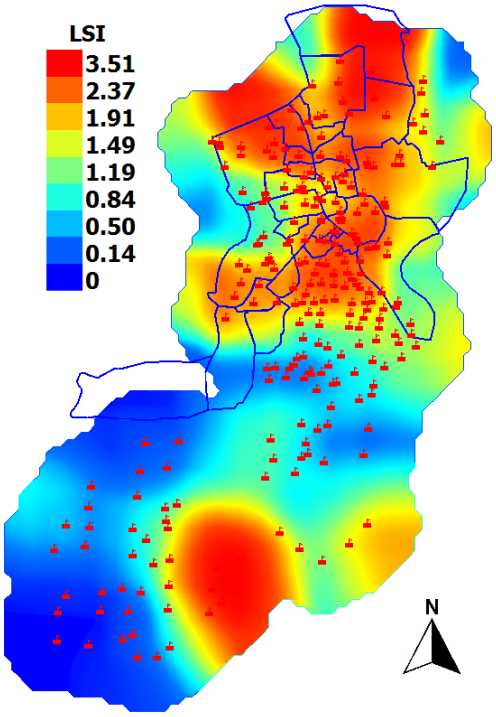

(a)

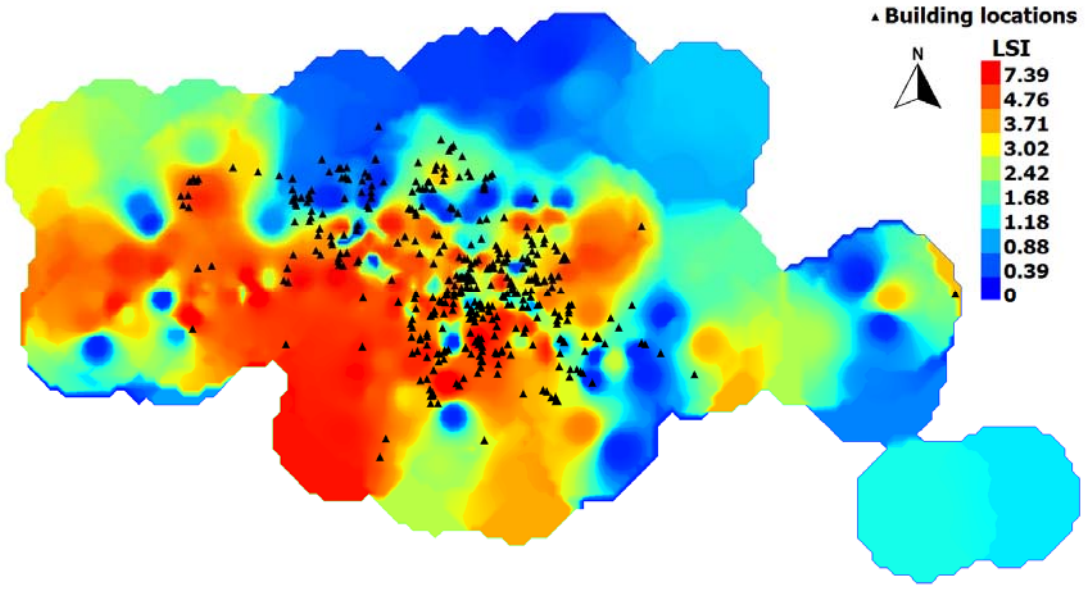

(b)

Figure 2.9. Liquefaction Severity Index contours in Adapazarı (a) and in Düzce (b).

Total strain was estimated by taking a weighted average of volumetric strain and deviatoric strain such that volumetric strain would contribute to 90% of total strain,

Total strain was estimated by taking a weighted average of volumetric strain and deviatoric strain such that volumetric strain would contribute to 90% of total strain, whereas deviatoric strain would contribute 10% of the strain. Total strain formulation, in which these weights are applied, is given in Equation 2.9. For each borehole; total settlement (S) was estimated in centimeters from total strain of liquefiable layers by multiplying liquefiable layers thickness with estimated total strain.

$$\text{Total Strain} = 0.9\,\varepsilon_v + 0.1\,\gamma \tag{2.9}$$

Through the years since the study of Yilmaz (2004), several new approaches and models were introduced for liquefaction induced settlement assessment. Liquefaction induced volumetric settlement model was updated by Çetin et al. (2009) in a study that uses maximum likelihood approach for developing a new model employing a database of more than 200 cases. They also reviewed previous settlement models by Wu and Seed (2004), Shamoto et al. (1998), Ishihara and Yoshimine (1992), Tokimatsu and Seed (1984). This newly developed volumetric settlement model was compared with case histories in the companion paper of Çetin et al. (2009) and it was concluded that this model gives superiorly accurate predictions for free field settlement. Therefore in this study, these models are updated with Çetin at al. (2009) volumetric strain model and only volumetric strain was considered in the analysis of liquefaction settlement.

Çetin at al. (2009) volumetric strain model requires fines correction for applied on overburden pressure corrected SPT values of $N_{1,60}$. Such a correlation was suggested by CEA2018 and it was implemented in this study. As the new correlation CEA2018 suggests in Figure 2.10, Equation 2.10 and 2.11 were employed in corrections for fines correction.

$$N_{1,60,CS} = N_{1,60} + \Delta N_{1,60} \tag{2.10}$$

$$\Delta N_{1,60} = FC \cdot (\,0.00167\,N_{1,60} + 0.089\,) \tag{2.11}$$

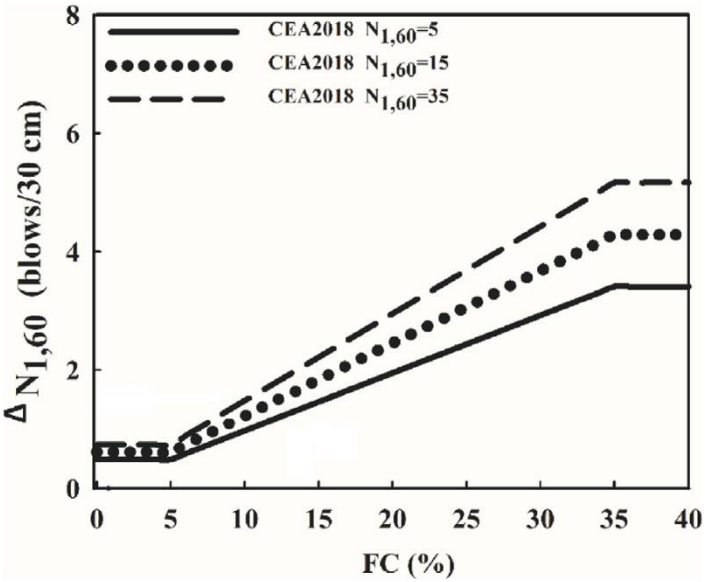

Figure 2.10. $N_{1,60,CS}$ correction parameter vs Fines Content (CEA2018)

For every depth level, $N_{1,60,CS}$ was determined in compliance with the CEA2018 method. Relative density was estimated from $N_{1,60,CS}$ values. For every standard penetration test depth; a corresponding D_R value was estimated using Idriss and Boulanger (2008) correlation between $N_{1,60,CS}$ and DR given in Equation 2.12.

$$D_R = \sqrt{\frac{N_{1,60,CS}}{46}} \tag{2.12}$$

Implementation of Çetin et al. (2009) volumetric settlement model requires 1 dimensional, 20 uniform loading cycles simple shear test CSR value ($CSR_{SS,20,1\text{-}D,1atm}$) as an input parameter. Unidirectionality factor (K_{md}), magnitude factor and stress scaling factor are computed in order to convert field CSR to $CSR_{SS,20,1\text{-}D,1atm}$.

Cyclic Stress Ratio was determined by Equation 2.1 as suggested by Seed and Idriss (1971). Unidirectionality Factor (K_{md}) is used to convert multi-directionally applied field CSR to a unidirectionally applied laboratory CSR. Its formulation is given in Equation 2.13.

$$K_{md} = 0.361 \ln(D_R) - 0.579 \tag{2.13}$$

Volumetric strain model by Çetin et al. (2009) is proposed for 20 uniform loading cycles. Therefore field CSR should be corrected for the magnitude and duration scaling. Magnitude factor proposed by Çetin et al. (2004) is given in Equation 2.14.

$$K_{M_w} = \frac{87.1}{{M_w}^{2.217}} \tag{2.14}$$

Finally, stress scaling factor, K_σ is employed so that nonlinear increase in cyclic resistance to shear stresses value is considered as well. K_σ correction in Equation 2.15 is suggested by Youd et al. (2001).

$$K_\sigma = (\frac{\sigma'_{v,0}}{P_a})^{-0.005 \cdot D_R} \tag{2.15}$$

After all correction factors are determined for each SPT depth, original field CSR values were converted to $CSR_{SS,20,1\text{-}D,1atm}$ values by Equation 2.16.

$$CSR_{\mathrm{SS,20,1-D,1atm}} = \frac{CSR_{field}}{K_{md} \cdot K_{M_w} \cdot K_\sigma} \tag{2.16}$$

As shown in Equation 2.17, volumetric strain of model by Çetin et al. (2009) is a function of fines corrected SPT value ($N_{1,60,CS}$) and 1 dimensional, 20 uniform loading cycles simple shear test CSR value($CSR_{SS,20,1\text{-}D,1atm}$) which is under a confinement pressure of 1 atm.

$$\ln(\varepsilon_v) = \ln\left\{1.879 \cdot \ln\left[\frac{780.416 \cdot \ln CSR_{\mathrm{SS,20,1-D,1atm}} - N_{1,60,CS} + 2442.465}{636.613 \cdot N_{1,60,CS} + 306.732}\right] + 5.583\right\} \pm 0.689 \tag{2.17}$$

Limitations of Çetin at al. (2009) volumetric strain model were employed for $N_{1,60,CS}$ and $CSR_{SS,20,1\text{-}D,1atm}$ in this model such that; $5 \leq N_{1,60,CS} \leq 40$ and $0.05 \leq CSR_{\mathrm{SS,20,1-D,1atm}} \leq 0.60$. For each borehole in database, volumetric strain for all cohesionless saturated soil layers was estimated with Equation 2.17.

Çetin at al. (2009) volumetric strain model also employs a depth factor (DF) for settlement in the equivalent volumetric strain formulation, such that depth factor diminishes with increasing depth (d_i) until critical depth of 18 meters. Depth factor

is also computed for every cohesionless saturated soil layer. Thus, an equivalent volumetric strain for each borehole was estimated via Equation 2.18 and 2.19.

$$DF_i = 1 - \frac{d_i}{z_{cr} = 18m} \tag{2.18}$$

$$\varepsilon_{v,eqv.} = \frac{\sum \varepsilon_{v,i} \cdot t_i \cdot DF_i}{\sum t_i \cdot DF_i} \tag{2.19}$$

Çetin at al. (2009) volumetric strain model also employs a depth factor (DF) for settlement in the equivalent volumetric strain formulation, such that depth factor soil layer as given in formulation by Çetin at al. (2009).

$$s_{estimated} = \varepsilon_{v,eqv.} \cdot \sum t_i \tag{2.20}$$

Estimated liquefaction settlements by Çetin at al. (2009) model show considerably different results compared with the previously employed model of Unutmaz and Çetin (2004). Settlement estimation change was under ±5 cm for 176 estimations out of 250 boreholes, whereas estimated liquefaction settlements increased more than 5 cm for 30 boreholes (Figure 2.11).

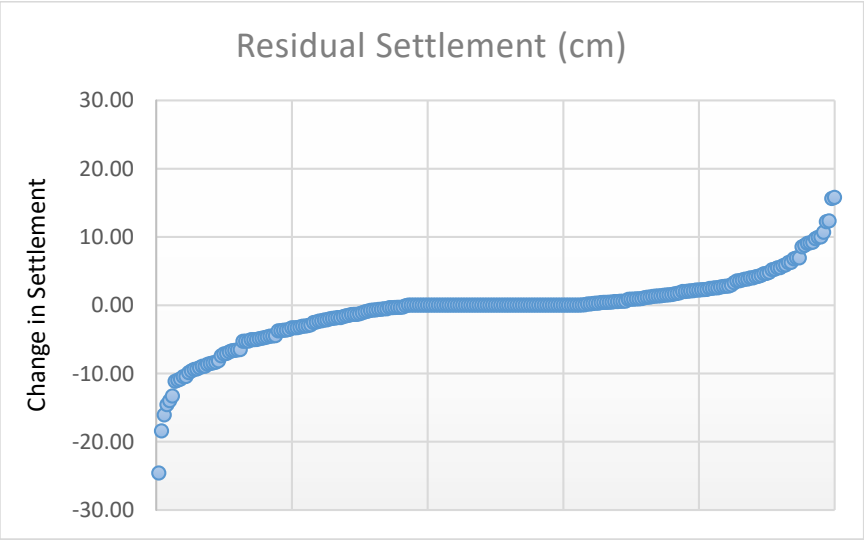

Figure 2.11. Residual Settlement (cm) comparing updated results of this study and Yilmaz (2004)

Liquefaction induced settlements (S) for each borehole was plotted using the GIS framework, and raster images are drawn using the inverse distance weighting method. Resulting contour maps are given in Figures 2.12 (a) and (b) along with central neighborhoods of Adapazarı and locations of buildings in Düzce within the dataset. Estimations of liquefaction induced settlement increased significantly when compared to the previous study of Yilmaz (2004). In the central neighborhoods of Adapazarı, this increase is more apparent than other regions to the south.

Depending on the locations of buildings; settlement and LSI values specific to building location are read and recorded. These updated values of settlement and LSI are combined with the number of floor, damage index and spectral acceleration information from 1-D site response analysis thus two final databases of Adapazarı and Düzce are shaped ready for statistical studies for damage prediction index modeling.

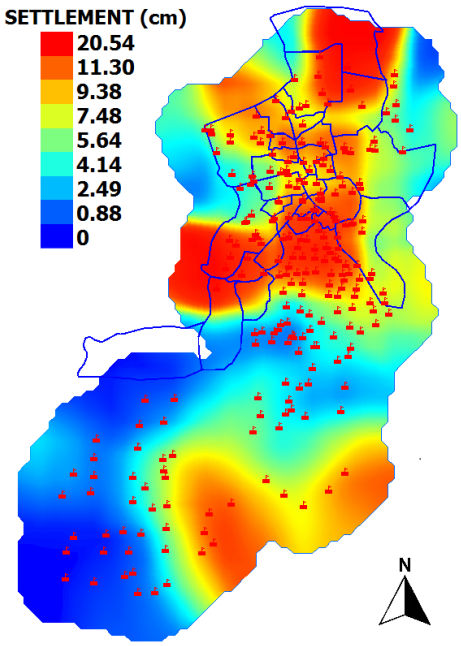

(a)

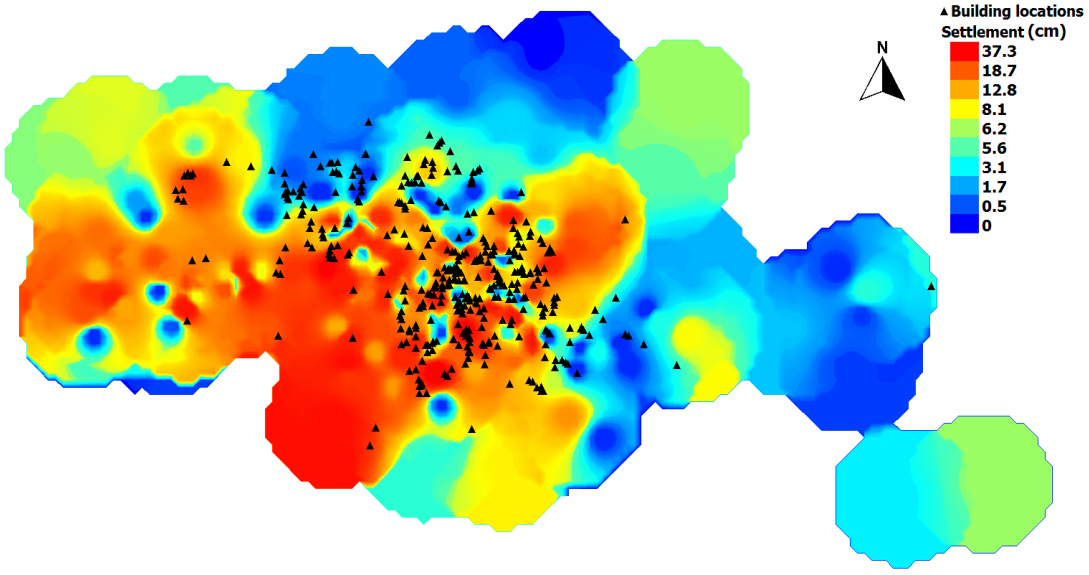

(b)

Figure 2.12. Liquefaction Induced Settlement Contours in Adapazarı (a) and in Düzce (b)

CHAPTER 3

DEVELOPMENT OF DAMAGE PREDICTION MODELS BASED ON GROUND MOTION AND GEOTECHNICAL PARAMETERS

In Chapter 2, two datasets were compiled for Adapazarı and Düzce cities which include the number of stories (N) for each building, ground motion parameters such as PGA and spectral accelerations (SA) at different spectral periods, geotechnical engineering parameters such as liquefaction severity index (LSI) and liquefaction-induced settlement in cm (S), and the damage states (G) for each building resulting after 1999 Düzce and Kocaeli earthquakes. The parameters in the datasets have different characteristics: G of the buildings and N are categorical variables (e.g. G may take the value of 1, 2 and 3 depending on the damage level); whereas PGA, SA, LSI and S are continuous variables. Therefore, standard regression analysis methods such as least-square regression are not suitable for the damage prediction models developed in this study. This chapter presents the statistical background for the selected model developing methods and summarizes the attempts to build the damage predication models that have a strong prediction performance. It should be noted that for every model presented in this chapter, the model coefficients are estimated for both datasets separately and then model performance was tested on each dataset to ensure the consistency in the model performance. In other words, when the model coefficients are estimated for the Adapazarı dataset, the model performance is tested by using Adapazarı and Düzce datasets individually and the combined dataset that includes data from both Adapazarı and Düzce.

3.1 Linear Discriminant Analysis Method

Initially, the linear discriminant analysis methods based on the general functional form given in Equation 3.1 is preferred to evaluate the relationship between the

damage state (G) and damage inducing variables. Linear discriminant analysis (LDA) finds the linear combination of features (such as damage inducing parameters) that characterizes or separates two or more classes of objects or events such as damage states. The resulting combination may be used as a linear classifier for classifying the data into one of the damage states. LDA method is suitable when the independent parameters are continuous and the dependent variable is categorical (Wetcher-Hendricks, 2011). On the other hand, LDA results in a continuous discriminant score for the damage prediction models developed in this study because the majority of the damage inducing parameters (PGA, SA, LSI and S) is continuous parameters. Therefore, the cutoff values (CV) have to be determined for separating resultant discriminant scores among the damage categories such that the number of miss-classified buildings in each category is minimized. In this study, the LDA is performed in SPSS software (IBM, 2011) to estimate θ_1-θ_6 and CVs are evaluated by maximizing the number of correct predictions in each damage category using maximum likelihood method.

$$g_{1-2-3} = \theta_1 \cdot N + \theta_2 \cdot PGA + \theta_3 \cdot SA + \theta_4 \cdot LSI + \theta_5 \cdot S + \theta_6 \quad (3.1)$$

3.2 Trial 1: Comparison of Tripartite and Bipartite Damage Categories

The Düzce database was also utilized in Yücemen et al. (2004) by considering two and three damage states for the same set of independent variables, showing that the overall correct classification rate is higher when two damage states was defined. Inspired by the previous efforts, Equation 3.1 is employed in the LDA by considering tripartite (none/light, moderate and severe) and bipartite (damaged/non-damaged) damage states and the model coefficients are estimated for Adapazarı and Düzce datasets, individually. Coefficients estimated by LDA for the tripartite damage states and the CVs separating none/light from moderate (CV_{1-2}) and moderate from severe (CV_{2-3}) damage states are given in Table 3.1.

Table 3.1. Coefficients of Equation 3.1 obtained by LDA and the CVs separating tripartite damage states using Adapazarı and Düzce datasets

Host Dataset	$\boldsymbol{\theta_1}$	$\boldsymbol{\theta_2}$	$\boldsymbol{\theta_3}$	$\boldsymbol{\theta_4}$	$\boldsymbol{\theta_5}$	$\boldsymbol{\theta_6}$	$\boldsymbol{CV_{1-2}}$	$\boldsymbol{CV_{2-3}}$
Adapazarı	0.13732	2.4343	-0.38606	0.21929	-0.013425	0.031528	1.3547	1.8359
Düzce	0.024783	2.0186	-0.18176	-0.035193	0.015994	0.69113	1.6730	1.8752

Correct classification ratios for the data in the host datasets for this initial trial are presented in Figure 3.1. This model results in a reasonable number of correct predictions for none/light (66% for Adapazarı, 52% for Düzce) and moderate (72% for Adapazarı, 52% for Düzce) damage cases. On the other hand, when the model is applied to tripartite damage states, the percentage of correct predictions in the severe damage state is significantly low (none for Adapazarı, 28% for Düzce). Because of the relative importance of the correct estimations in the severe damage state with respect to the other damage states, bipartite damage states are utilized in LDA, based on the model form given in Equation 3.2.

$$g_{1-2} = \theta_1 \cdot N + \theta_2 \cdot PGA + \theta_3 \cdot SA + \theta_4 \cdot LSI + \theta_5 \cdot S + \theta_6 \tag{3.2}$$

Equation 3.2 is similar to Equation 3.1, except that only one CV is required to distinguish between damaged and non-damaged states (CV_{1-2}). Coefficients estimated by LDA for Adapazarı and Düzce datasets for the bipartite damage states and CV_{1-2} are given in Table 3.2.

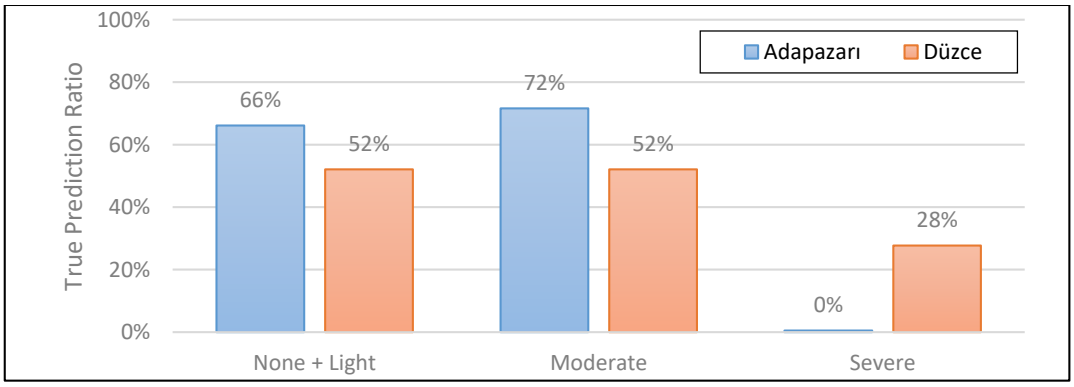

Figure 3.1. True prediction ratios of linear discriminant and tripartite category model (Equation 3.1)

Table 3.2. Coefficients of Equation 3.2 obtained by LDA and the CVs separating bipartite damage states using Adapazarı and Düzce datasets

Host Dataset	$\boldsymbol{\theta_1}$	$\boldsymbol{\theta_2}$	$\boldsymbol{\theta_3}$	$\boldsymbol{\theta_4}$	$\boldsymbol{\theta_5}$	$\boldsymbol{\theta_6}$	$\boldsymbol{CV_{1-2}}$
Adapazarı	0.10432	1.7019	-0.24115	0.15046	-0.0093775	0.26964	1.2391
Düzce	-0.06369	0.65931	-0.23642	0.037894	-0.011853	1.8314	1.5488

To evaluate the predictive power of Equation 3.2, model coefficients derived by using the Adapazarı dataset is tested by calculating the correct classification ratios for the individual Adapazarı and Düzce datasets in addition to the combined dataset as shown in Figure 3.2. Düzce databases predict their own damage cases moderately well. As presented in Figure 3.2 and 3.3, both of these models are cross checked with their counterpart database and combined database of both cities. It is observed that Adapazarı origin linear discriminant model has a decent agreement with the actual damage states in Düzce test database, especially for the damaged building cases. Similarly, Düzce origin model is also predicting actual damage observed in Adapazarı test database considerably well for the damaged cases.

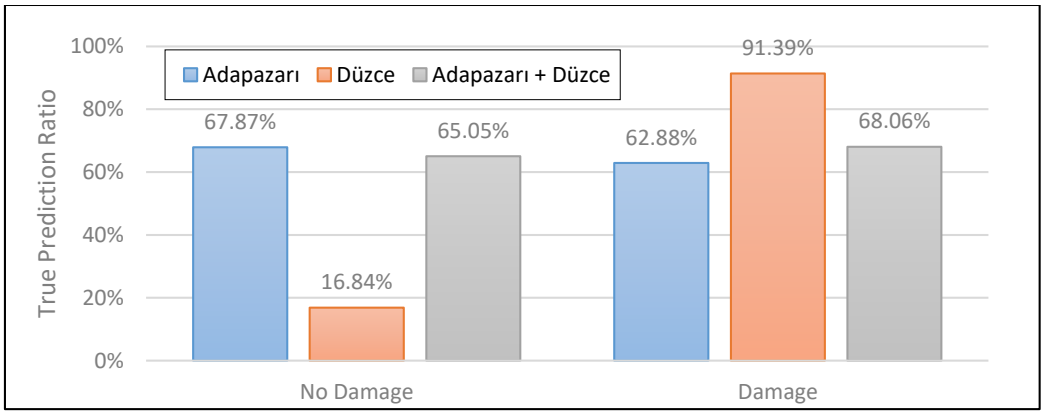

Figure 3.2. True prediction ratios of linear discriminant and bipartite category model derived from Adapazarı origin database (Equation 3.2)

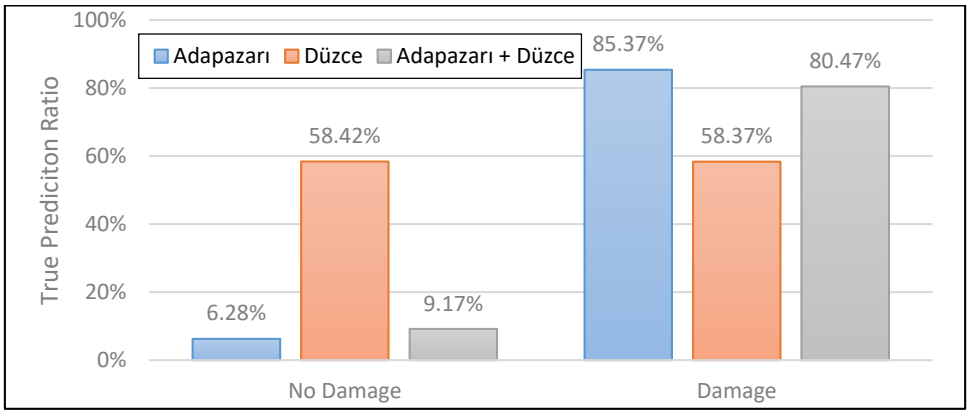

Figure 3.3. True prediction ratios of linear discriminant and bipartite damage category model derived from Düzce origin database (Equation 3.2)

3.3 Trial 2: Individual Contributions of Dependent Parameters

In their work, Askan and Yücemen (2010) had also studied Düzce city after 1999 Düzce Earthquake. Building cases had been examined under quadripartite damage categories and only structural damage inducing parameters had been considered. It was assumed that all building inventory was exposed to same earthquake and same soil conditions. True prediction ratios of Askan and Yücemen (2010) linear discriminant model was 61.0%, 49.3%, 23.8% and 60.9% for damage cases of none, light, moderate and severe, while overall true prediction ratio was 50.7% for whole

Düzce database. Only common parameter of this study and Askan and Yücemen (2010), considered as a damage inducing parameter is number of storeys (N). This parameter is separately examined and evaluated using a univariate discriminant analysis in Equation 3.3.

$$g_{1-2} = \theta_1 \cdot N + \theta_2 \tag{3.3}$$

Results of this univariate discriminant analysis suggests that using only N as a damage inducing parameter, damaged buildings and non-damaged buildings can be predicted suitably. Discriminant coefficients and true prediction ratios of this model are given in Table 3.3 and Figure 3.4. Model derived from Düzce origin database has an 80.38% true prediction ratio for damaged cases, whereas Adapazarı database originated model has 64.48% true prediction ratio. When these two separate database originated models are assessed with their test databases, same true prediction ratios are observed. In other words, both Adapazarı city and Düzce city originated models are predicting other city with same true prediction ratios.

Table 3.3. Discriminant coefficients for model with single parameter of number of storey (Equation 3.3)

Host Dataset	$\boldsymbol{\theta_1}$	$\boldsymbol{\theta_2}$	$\boldsymbol{CV_{1-2}}$
Adapazarı	0.11543	0.80638	1.2391
Düzce	0.13130	0.99004	1.5153

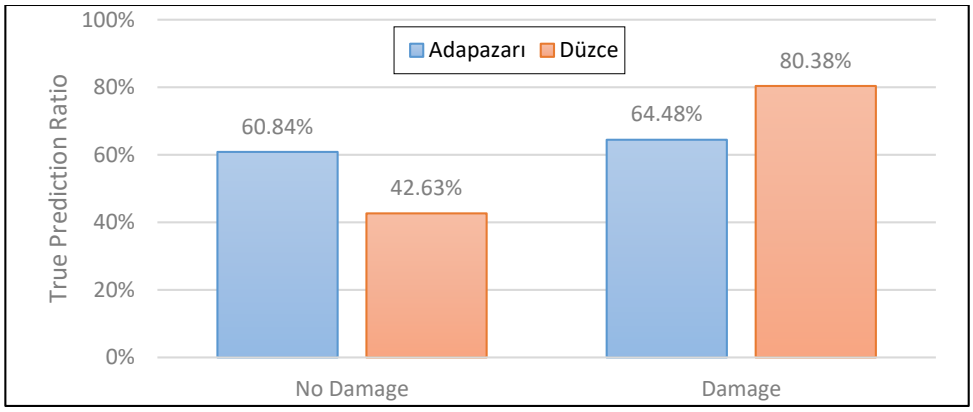

Figure 3.4. True prediction ratios of linear discriminant models using only number of storey as parameter (Equation 3.3)

3.4 Contribution of Earthquake Parameters

Moving on from the results of univariate discriminant analysis, distinct contributions of earthquake and liquefaction parameters are compared. Initially, contribution of earthquake parameters was investigated by using only three damage inducing variables: PGA, SA and N. Discriminant analysis is performed for the damage model in Equation 3.4 and its results are given in Table 3.4. True prediction ratios for both origin database and test database for two separate models, derived from Adapazarı and Düzce origin databases are given in Figure 3.5 and Figure 3.6 respectively. Both prediction models originated from Adapazarı and Düzce cities are predicting their origin databases with a reasonable true ratio of 64.85% - 61.93% and 59.47% and 59.81% for no damage and damaged cases for respective cities. On the contrary, both models are poorly predicting test databases of opposite cities as no damage category true prediction ratios are 0% and 1.36% for two models.

$$g_{1-2} = \theta_1 \cdot N + \theta_2 \cdot PGA + \theta_3 \cdot SA + \theta_4 \tag{3.4}$$

Table 3.4. Discriminant coefficients for earthquake parameters and number of storey (Equation 3.4)

Host Dataset	$\boldsymbol{\theta_1}$	$\boldsymbol{\theta_2}$	$\boldsymbol{\theta_3}$	$\boldsymbol{\theta_4}$	$\boldsymbol{CV_{1-2}}$
Adapazarı	0.10938	2.2857	-0.17958	0.26008	1.2436
Düzce	-0.06319	0.66494	-0.23579	1.8030	1.5153

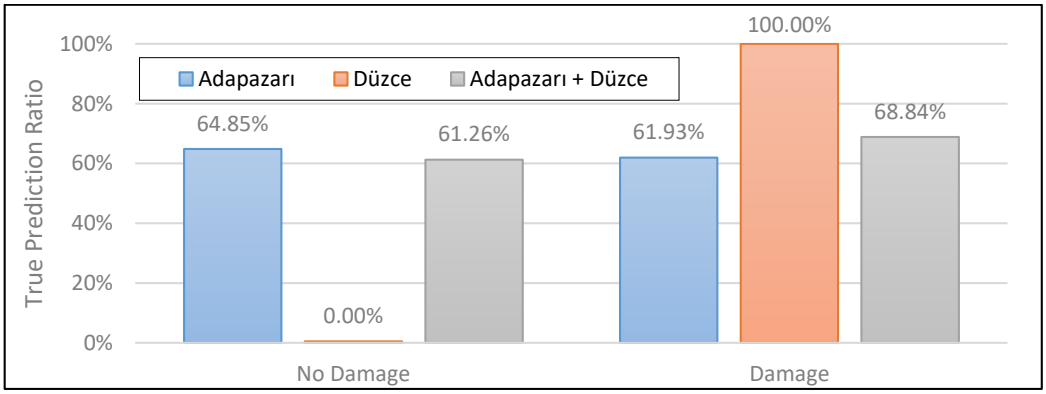

Figure 3.5. True prediction ratios of prediction model derived from Adapazarı database (Equation 3.4)

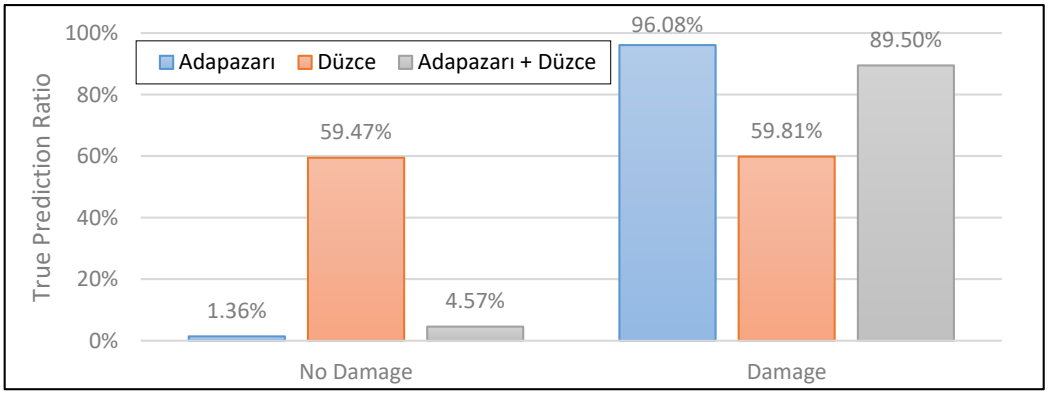

Figure 3.6. True prediction ratios of prediction model derived from Düzce database (Equation 3.4)

3.5 Contribution of Liquefaction Parameters

Contribution of liquefaction parameters to damage are assessed secondly, using three damage inducing parameters of N, LSI and S. Discriminant analysis is performed for the damage model in Equation 3.5 and its results are given in Table 3.5. True prediction ratios for both origin database and test database for two separate models, derived from Adapazarı and Düzce origin databases are given in Figure 3.7 and Figure 3.8 respectively. Düzce database originated prediction model has 59.47% and 58.85% true prediction ratios for its origin database, while this model has 84.04% and 33.62% true prediction ratios for the test model of Adapazarı database. Since true prediction ratios of model of Equation 3.5 is better than model of Equation 3.4, it is observed that liquefaction parameters of LSI and S have higher positive contribution to true prediction ratios compared to earthquake parameters of PGA and SA.

$$g_{1-2} = \theta_1 \cdot N + \theta_2 \cdot LSI + \theta_3 \cdot S + \theta_4 \tag{3.5}$$

Table 3.5. Discriminant coefficients for liquefaction parameters and number of storey (Equation 3.5)

Host Dataset	$\boldsymbol{\theta_1}$	$\boldsymbol{\theta_2}$	$\boldsymbol{\theta_3}$	$\boldsymbol{\theta_4}$	$\boldsymbol{CV_{1-2}}$
Adapazarı	0.11119	0.15563	-0.0093665	0.60238	1.2170
Düzce	0.13155	0.050118	-0.014304	1.0023	1.5154

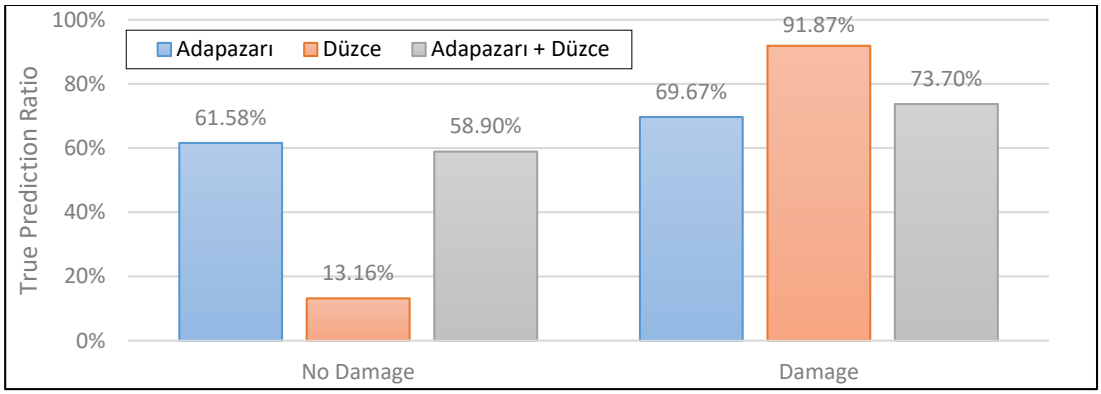

Figure 3.7. True prediction ratios of prediction model derived from Adapazarı database (Equation 3.5)

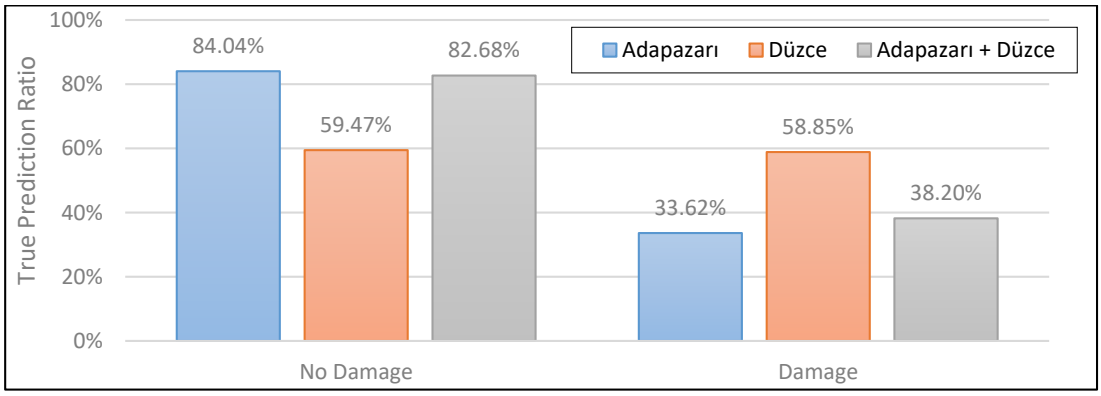

Figure 3.8. True prediction ratios of prediction model derived from Düzce database (Equation 3.5)

3.6 Trial 3: Prediction Models with Exponential Parameters

Among the damage inducing parameters, most influential parameter was observed to be N by testing in Equation 3.3. For the next phase of discriminant analysis, the exponential term of number of storeys is introduced into the model by Equation 3.6 and results are presented in Table 3.6. True prediction ratios for both origin database and test database for two separate models, derived from Adapazarı and Düzce origin databases are given in Figure 3.9 and Figure 3.10 respectively. Adapazarı originated model results in 53.45% and 71.69% true predictions for its origin database,

moreover; this model results in 56.84% and 56.46% true predictions for test database of Düzce city. Changing the number of storey term into its exponential self, resulted in an improvement for predictions for test database.

$$g_{1-2} = \theta_1 \cdot e^N + \theta_2 \cdot PGA + \theta_3 \cdot SA + \theta_4 \cdot LSI + \theta_5 \cdot S + \theta_6 \quad (3.6)$$

Table 3.6. Discriminant coefficients for Equation 3.6

Host Dataset	$\boldsymbol{\theta_1}$	$\boldsymbol{\theta_2}$	$\boldsymbol{\theta_3}$	$\boldsymbol{\theta_4}$	$\boldsymbol{\theta_5}$	$\boldsymbol{\theta_6}$	$\boldsymbol{CV_{1-2}}$
Adapazarı	- 4.0528E-10	3.9392	-1.1661	0.16388	-0.0089166	0.44471	1.2272
Düzce	-3.9802E-4	0.55607	-0.19673	0.036337	-0.011303	1.5959	1.5535

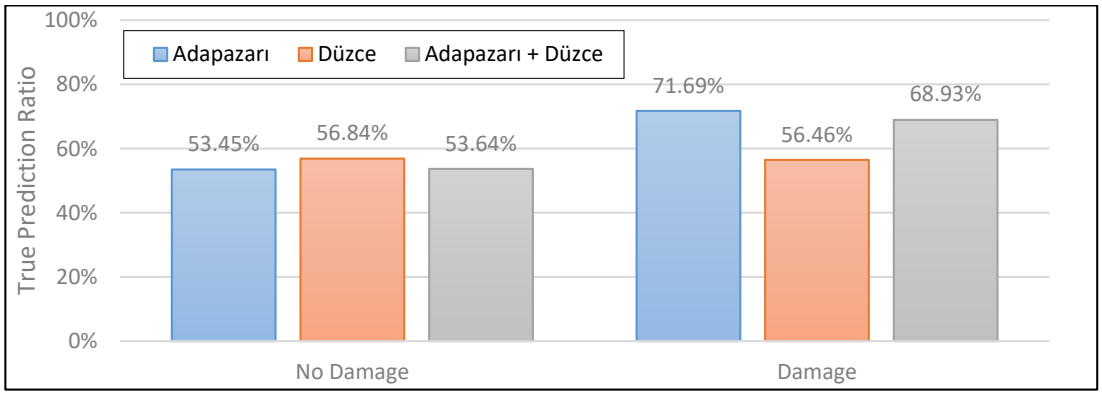

Figure 3.9. True prediction ratios of prediction model derived from Adapazarı database (Equation 3.6)

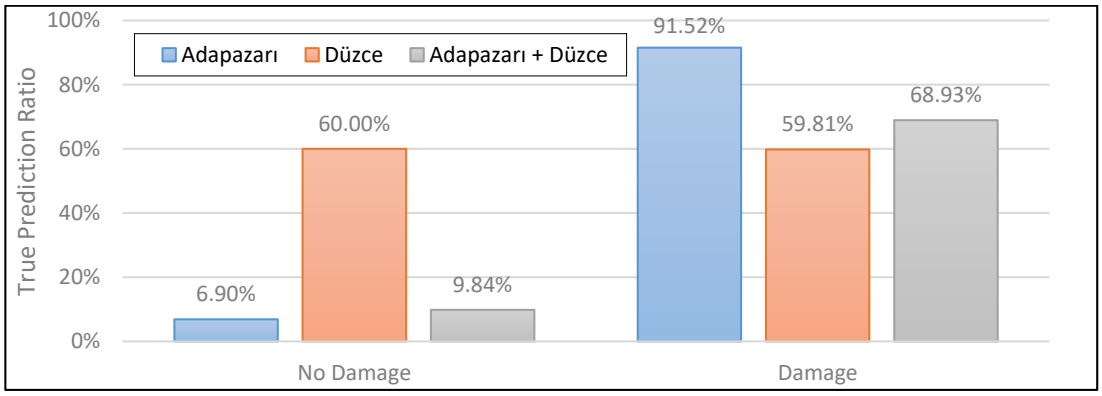

Figure 3.10. True prediction ratios of prediction model derived from Düzce database (Equation 3.6)

By combining origin databases of Adapazarı and Düzce, another linear discriminant model is developed finally using exponential of number of storeys and LSI, S, PGA and SA as damage inducing parameters in Equation 3.6. Discriminant coefficients for the combined database of Adapazarı and Düzce is given in Table 3.7. True prediction ratios for combined origin database and individual test databases are given in Figure 3.11. Resulting true predictions show that this combined model is predicting all individual databases reasonably well.

Table 3.7. Discriminant coefficients for Equation 3.6 using combined database

Host Dataset	$\boldsymbol{\theta_1}$	$\boldsymbol{\theta_2}$	$\boldsymbol{\theta_3}$	$\boldsymbol{\theta_4}$	$\boldsymbol{\theta_5}$	$\boldsymbol{\theta_6}$	$\boldsymbol{CV_{1-2}}$
Adapazarı + Düzce	0.24739	0.33980	-0.32488	0.52842	-1.0994	0.46482	1.2275

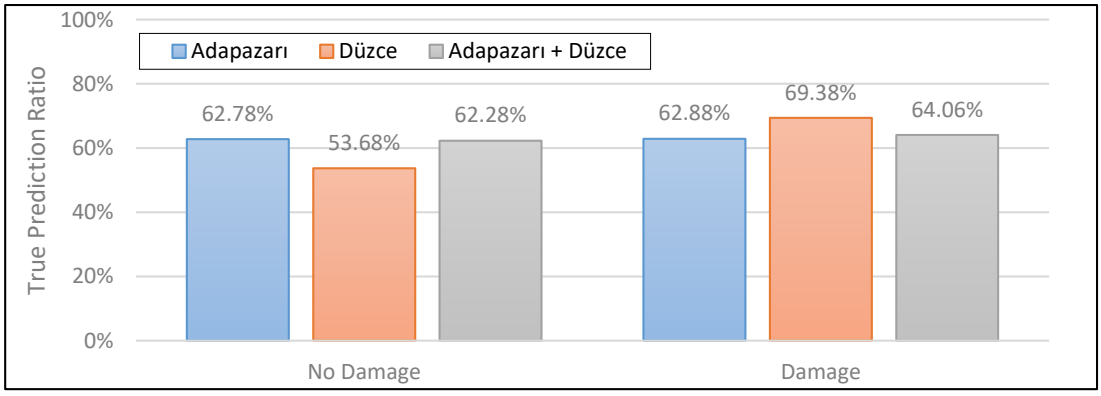

Figure 3.11. True prediction ratios of prediction model derived from Adapazarı + Düzce combined database (Equation 3.6)

3.7 Multinomial Logistics Regression

Another statistical approach for categorizing damage states using a set of independent damage inducing parameters is multinomial logistics regression. Logistics regression is a useful tool especially for categorical dependent values such as damage index. Rather than comparing discriminant scores with cutoff values, as performed in discriminant analysis method; logistics regression returns the

probability of damage for each case in the regression database and results in logarithm of odds of a certain damage index category. Multinomial logistics regression analysis was performed for Adapazarı and Düzce origin databases using the model of Equation 3.7. Logistics regression formula can be rephrased as Equation 3.8 for evaluation of damage probability as well. Coefficients of multinomial logistics regression for Adapazarı and Düzce database origin models are given in Table 3.8. True prediction ratios for combined and individual origin database databases are given in Figure 3.12 and 3.13. Multinomial regression model results in poor estimations for both origin database and test database for both Adapazarı and Düzce database originated models.

$$Logit = \ln\left[\frac{P(g=2)}{1-P(g=2)}\right] = \theta_1 \cdot e^N + \theta_2 \cdot PGA + \theta_3 \cdot SA + \theta_4 \cdot LSI + \theta_5 \cdot S + \theta_6 \quad (3.7)$$

$$P(g=2) = 1/(1 + e^{-\theta_1 \cdot e^N - \theta_2 \cdot PGA - \theta_3 \cdot SA - \theta_4 \cdot LSI - \theta_5 \cdot S - \theta_6}) \quad (3.8)$$

Table 3.8. Multinomial regression coefficients for Equation 3.7 and 3.8

Host Dataset	$\boldsymbol{\theta_1}$	$\boldsymbol{\theta_2}$	$\boldsymbol{\theta_3}$	$\boldsymbol{\theta_4}$	$\boldsymbol{\theta_5}$	$\boldsymbol{\theta_6}$
Adapazarı	0.0059465	12.058	-2.2790	1.0060	-0.060094	-5.3797
Düzce	-0.0016471	2.3120	-0.81326	0.15580	-0.048458	0.39051

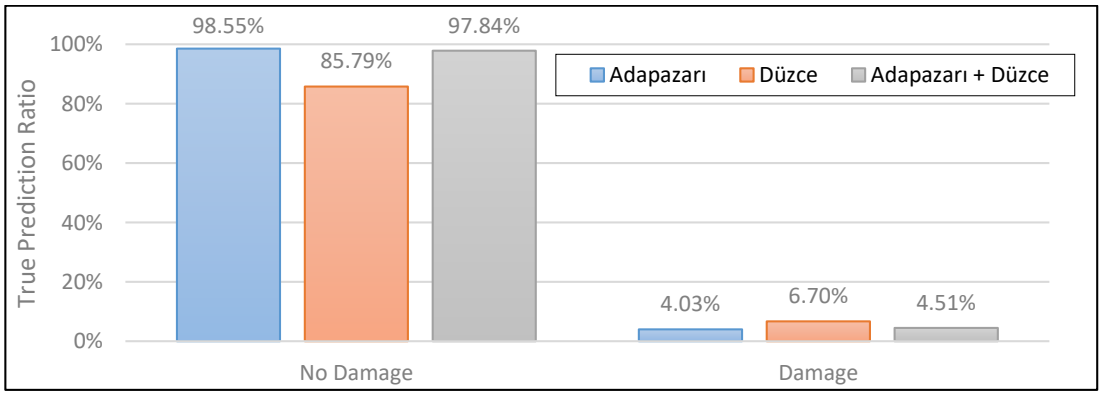

Figure 3.12. True prediction ratios of logistics regression model derived from Adapazarı origin database (Equation 3.7)

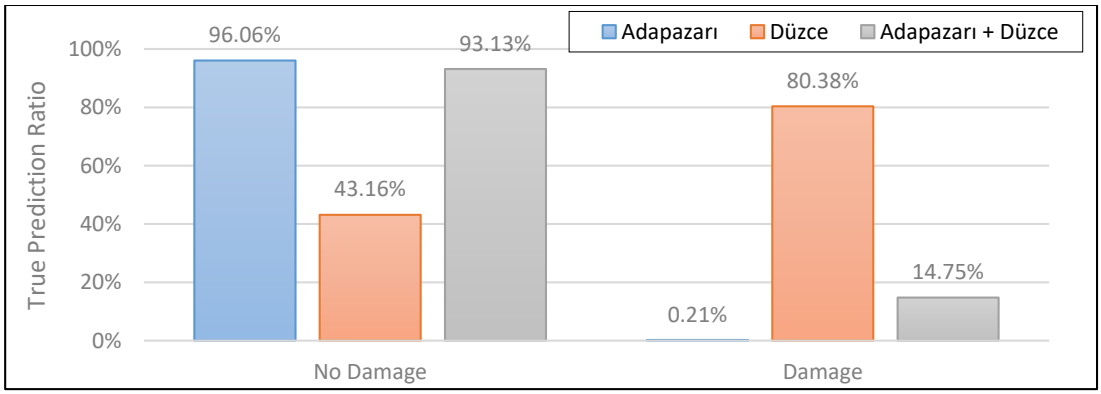

Figure 3.13. True prediction ratios of logistics regression model derived from Düzce origin database (Equation 3.7)

Multinomial logistic regression results in very poor damage prediction for both models developed over Düzce and Adapazarı databases. This regression method is giving poor results, such as less than 5% true prediction for Adapazarı database, mostly due to the imbalanced distribution of damaged and non-damaged cases in Adapazarı database. Although Düzce database originated model results in relatively better results, resulting in 43.16% no damage case true predictions and 80.38% damage case true predictions, this results are not adequate when compared with results of previous models developed using discriminant analysis.

3.8 Maximum Likelihood Regression

Damage inducing parameters such as LSI, S, PGA and SA are normally distributed parameters. Therefore resulting scores from linear regression should also have normally distribution. Evaluation of the mean resultant score (β) and its standard deviation (σ), allows probabilistic assessment of individual cases in terms of damage and no-damage. By maximizing total of logarithms of true damage category classification probabilities, maximum log likelihood regression is performed for Adapazarı and Düzce origin databases in order to assess if performance of prediction models can be improved. The model of Equation 3.9 is selected for first maximum likelihood regression analysis and coefficients summarized in Table 3.9 are obtained.

$$g_{1-2} = \theta_1 \cdot e^N + \theta_2 \cdot PGA + \theta_3 \cdot SA + \theta_4 \cdot LSI + \theta_5 \cdot S + \theta_6 \quad (3.9)$$

Results of maximum likelihood regression analysis and coefficients for Equation 3.9 is summarized in Table 3.9. True prediction ratios of Adapazarı and Düzce database originated models are given in Figure 3.16 and 3.17. It is observed that model of Equation 3.9 derived from Adapazarı database has an agreeable performance of projection for its origin database and test database since this model predicts its origin database by 66.48% and 58.43% for no damage and damage cases respectively. When checked with the test database, Adapazarı database originated model of Equation 3.9, results are also compliant with actual damage cases since 79.43% of damaged building cases are predicted accurately. However when compared with the linear discriminant model of Equation 3.6, true prediction ratios of maximum likelihood model are staying a little behind the true prediction ratios of linear discriminant model.

Table 3.9. Maximum likelihood coefficients for Equation 3.9

Host Dataset	$\boldsymbol{\theta_1}$	$\boldsymbol{\theta_2}$	$\boldsymbol{\theta_3}$	$\boldsymbol{\theta_4}$	$\boldsymbol{\theta_5}$	$\boldsymbol{\theta_6}$	σ	β
Adapazarı	0.00077172	1.6332	-0.32832	0.14320	-0.0090435	0.46922	0.19827	1.0257
Düzce	-0.00039802	0.55607	-0.19673	0.036337	-0.011303	1.5959	0.12273	1.5535

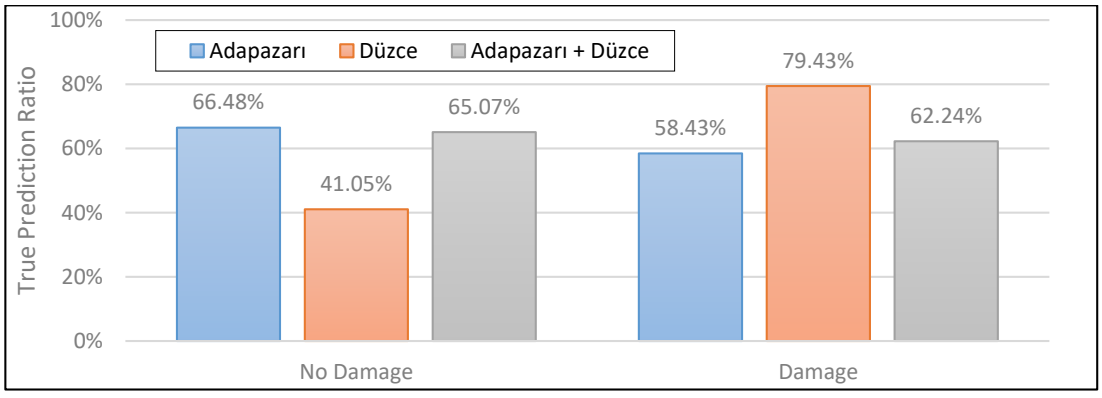

Figure 3.14. True prediction ratios of logistics regression model derived from Adapazarı origin database (Equation 3.9)

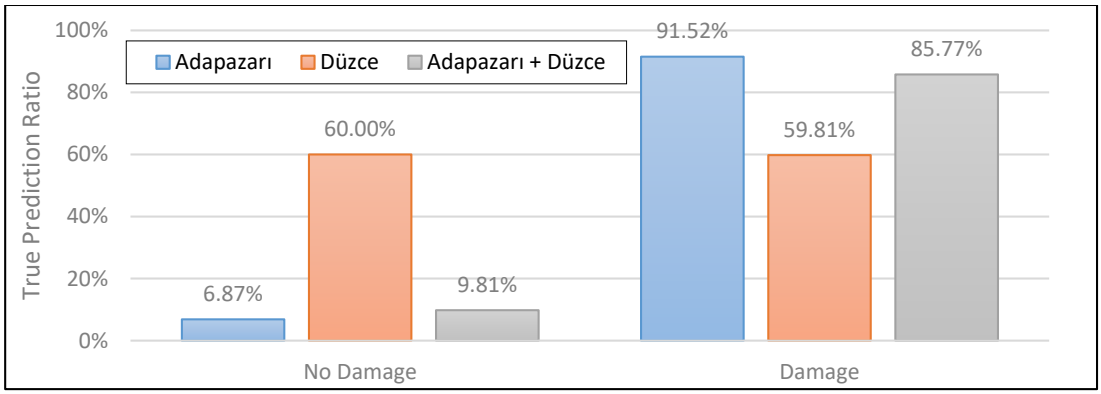

Figure 3.15. True prediction ratios of logistics regression model derived from Düzce origin database (Equation 3.9)

Maximum likelihood method benefits from the normal distribution of independent variables. Since damage inducing earthquake parameters of SA and PGA are log normally distributed; a model including log-normal values of these parameters is also considered in Equation 3.10. Maximum likelihood coefficients and regression parameters are given in Table 3.10 for model of Equation 3.10.

$$g_{1-2} = \theta_1 \cdot e^N + \theta_2 \cdot \ln PGA + \theta_3 \cdot \ln SA + \theta_4 \cdot LSI + \theta_5 \cdot S + \theta_6 \qquad (3.10)$$

Table 3.10. Maximum likelihood coefficients for Equation 3.10

Host Dataset	$\boldsymbol{\theta_1}$	$\boldsymbol{\theta_2}$	$\boldsymbol{\theta_3}$	$\boldsymbol{\theta_4}$	$\boldsymbol{\theta_5}$	$\boldsymbol{\theta_6}$	σ	β
Adapazarı	0.00076843	0.45830	-0.14933	0.13970	-0.0087680	1.4483	0.19492	1.2276
Düzce	-0.00024667	0.15471	-0.13702	0.019997	-0.0056073	1.8311	0.15616	1.6601

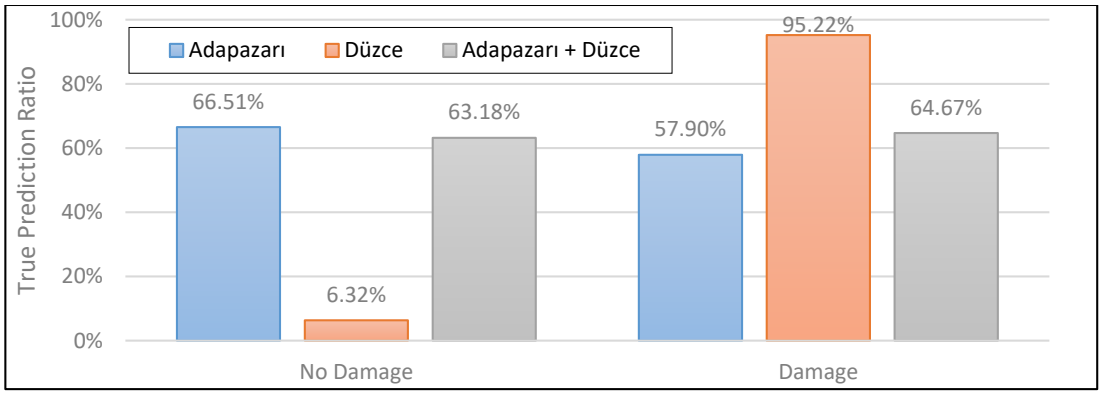

Figure 3.16. True prediction ratios of logistics regression model derived from Adapazarı origin database (Equation 3.10)

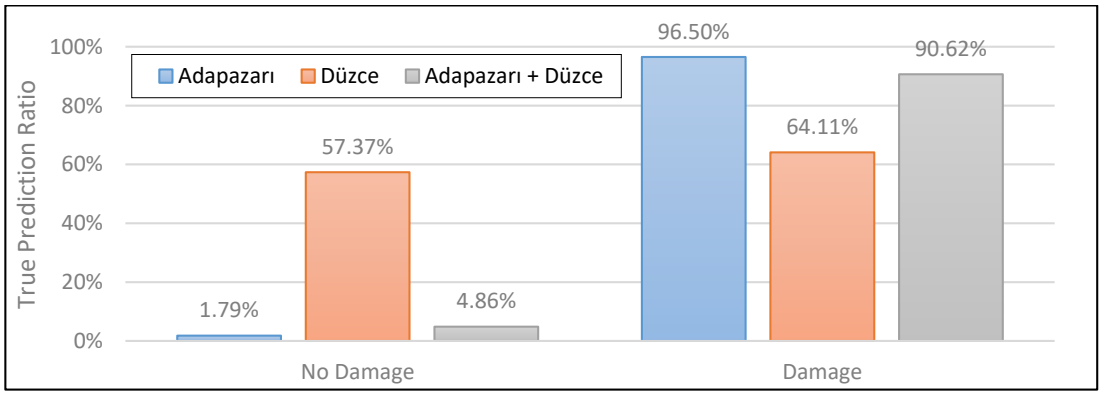

Figure 3.17. True prediction ratios of logistics regression model derived from Düzce origin database (Equation 3.10)

True prediction ratios of Adapazarı and Düzce database originated models are given in Figure 3.18 and 3.19. Both Adapazarı and Düzce originated models have good agreement with their origin databases, having true ratio of 66.51% - 57.90% and 57.37% and 64.11% for no damage and damaged cases for respective cities. However, performance of this model is weak when tested with the corresponding other database, since true predictions for no damage cases are 6.32% and 1.79% for no damage cases. When compared with the linear discriminant model of Equation 3.6, which is the best model evaluated so far, Equation 3.9 and 3.10 are resulting in inferior prediction of damage in most cases in their test databases. Maximum likelihood approach is resulting in accurate models similar to the linear discriminant

models, however linear discriminant models still have better true predictions because discriminant analysis method is selecting better cutoff values for the categorical output variable of G, maximizing number of true predictions.

CHAPTER 4

CONCLUSION

After 1999 Düzce and Kocaeli Earthquakes, damage prediction models were developed and tested for Düzce, Kaynaşlı and Erzincan. These damage prediction models were predicting 60-65% of damage levels correctly. However, these models were employing damage inducing parameters generally related to structural dimensions and design of structural frame. In current literature, damage prediction models that include geotechnical earthquake parameters is rare. Initial attempt to include geotechnical earthquake parameters within damage prediction models were performed by preliminary studies of Yilmaz and Çetin (2003) and Yilmaz (2004) using comprehensive database of Adapazarı. It was observed that approximately 60-65% of the damage states in Adapazarı database were predicted correctly by the proposed model with geotechnical earthquake parameters.

Improvements were introduced in geotechnical earthquake engineering parameters in the last decade. In this study, preliminary database of Adapazarı developed by Yilmaz (2004) was updated in terms of these liquefaction-related predictive parameters. In order to develop a second consistent database, 1-D site-specific ground response analyses were performed for the simplified soil models representing the boreholes in Düzce hence, a second database was compiled using AFAD's Düzce dataset collected after the 1999 Düzce earthquake. Thus, two consistent independent databases were compiled ready for damage model developing studies. Using Adapazarı and Düzce databases, models were developed from one origin database and tested with the other database and combined database of two. Better applicability and accuracy of these damage prediction models were aimed.

The damage prediction models are developed for both compiled databases using three statistical methods, linear discriminant analysis, multinomial logistics

regression and maximum likelihood methodology. Model performance is evaluated by analyzing the percentage of true predictions in the origin database and in the test database. Damage inducing parameters were assessed for their contribution to the final damage state by comparing a series of damage models. It was concluded that, common parameter of number of storey has a good agreement with damage states without any additional parameters. Earthquake parameters and liquefaction parameters are exclusively involved in follow up models to assess their contribution. True prediction ratios of models suggested that liquefaction parameters (LSI, S) had a better agreement (+10%-15%) with damage states when compared to earthquake parameters (PGA, SA). Models derived using multinomial statistical method and maximum likelihood models had slightly worse performance than discriminant models.

Discriminant model in Equation 4.1 and 4.2 have resulted in best performance of correct damage state prediction among all the models evaluated, resulting in 62.28% and 64.06% true predictions for no damage and damage states. Equation 4.1 is originated from Adapazarı database, whereas Equation 4.2 is derived using collective database of Adapazarı and Düzce. Performance of these two models indicate that the preliminary model proposed by Yılmaz (2004) is improved, especially in predicting the damaged cases.

$$g_{1-2} = -4.0528\text{E}-10 \cdot e^{N} + 3.9392 \cdot PGA - 1.1661 \cdot SA + 0.16388 \cdot LSI - -0.0089166 \cdot S + 0.44471, \quad CV = 1.2272 \tag{4.1}$$

$$g_{1-2} = 0.24739 \cdot e^{N} + 0.33980 \cdot PGA - 0.32488 \cdot SA + 0.52842 \cdot LSI - 1.0994 \cdot S + 0.46482, \quad CV = 1.2275 \tag{4.2}$$

Damage prediction model expressed by Equation 4.2 has a higher rate of true prediction for both databases, therefore model would give more precise results for further studies. Precision of models may be improved using data from future earthquakes, introduction of structural parameters would also result in better performance of prediction models.

REFERENCES

Askan, A., and Yucemen, M. S. (2010). Probabilistic methods for the estimation of potential seismic damage : Application to reinforced concrete buildings in Turkey. Structural Safety, 32(4), 262–271.

Aydan, Ö., Hamada, M., Bardet, J. P., Ulusay, R., & Kanibir, A. (2004, August). Liquefaction induced lateral spreading in the 1999 Kocaeli earthquake, Turkey: case study around the Hotel Sapanca. In Proceedings of the 13th world conference on earthquake engineering, Vancouver, BC, Canada, paper (No. 2921).

Boore, D. M., Joyner, W. B. and Fumal, T. E. (1997) ‘‘Equations for estimating horizontal response spectra and peak acceleration from Western North American earthquakes: a summary of recent work,’’ Seismological Research Letters 68(1), 128–153.

Boulanger RW and Idriss IM. CPT and SPT based liquefaction triggering procedures. (Report No. UCD/CGM-14/01). Davis, CA: Center for Geotechnical Modeling, Department of Civil and Environmental Engineering, University of California; 2014. p. 134.

Campbell, K. W. (1997) ‘‘Empirical near-source attenuation of horizontal and vertical component of peak ground acceleration, peak ground velocity, and pseudo-absolute acceleration response spectra,’’ Seismological Research Letters 68(1), 154–179.

Cetin, K. O., Youd, T. L., Seed, R. B., Bray, J. D., Sancio, R., Lettis, W., ... & Durgunoglu, H. T. (2002). Liquefaction-induced ground deformations at Hotel Sapanca during Kocaeli (Izmit), Turkey earthquake. Soil Dynamics and Earthquake Engineering, 22(9-12), 1083-1092.

Cetin, K. O., Seed, R. B., Der Kiureghian, A., Tokimatsu, K., Harder, L. F., Kayen, R. E., and Moss, R. E. S. (2004). Standard penetration test-based probabilistic and deterministic assessment of seismic soil liquefaction potential, J. Geotechnical and Geoenvironmental Eng., ASCE 130(12), 1314–340.

Cetin, K Onder, Bilge, H. T., Wu, J., Kammerer, A. M., and Seed, R. B. (2009). Probabilistic Model for the Assessment of Cyclically Induced Reconsolidation „ Volumetric Settlements. 135(3), 387–398. https://doi.org/10.1061/(ASCE)1090-0241(2009)135

Cetin, K Onder, Seed, R. B., Kayen, R. E., Moss, R. E. S., Bilge, H. T., and Ilgac, M. (2018). MethodsX The use of the SPT-based seismic soil liquefaction triggering evaluation methodology in engineering hazard assessments. MethodsX, 5, 1556–1575.

Cetin, K Onder, Seed, R. B., Kayen, R. E., Moss, R. E. S., Bilge, H. T., Ilgac, M., and Chowdhury, K. (2018). SPT-based probabilistic and deterministic assessment of seismic soil liquefaction triggering hazard. (July 2017).

Cetin, Kemal Onder. (2015). SPT - Based Probabilistic Assessment of Seismic Soil Liquefaction Initiation Hazard. (May).

Crowley, H., Pinho, R., and Bommer, J. J. (2004) ‘‘A probabilistic displacement-based vulnerability assessment procedure for earthquake loss estimation,’’ Bulletin of Earthquake Engineering 2(2), 173–219.

Dashti, S., Bray, J. D., Pestana, J., Riemer M. and Wilson D. (2010). Mechanisms of Seismically Induced Settlement of Buildings with Shallow Foundations on Liquefiable Soil. Journal of Geotechnical and Geoenvironmental Engineering, (January), 151–164.

Dickenson, S. E. (1994), “Dynamic Response of Soft and Deep Cohesive Soils During the Loma Prieta Earthquake of October 17, 1989”, Dissertation Submitted in Partial Satisfaction of the Requirements for the Degree of Doctor of Philosophy, University of California at Berkeley.

Dobry, R. and Vucetic, M. (1987), “Dynamic Properties and Seismic Response of Soft Clay Deposits”, Proceedings, International Symposium on Geotechnical Engineering of Soft Soils, Mexico City, Vol.2, pp.51-87.

Erberik, M. A. (2008a). Generation of fragility curves for Turkish masonry buildings considering in-plane failure modes, Earthquake Eng. Struct. Dynam. 37,

387–405.

Erberik, M. A. (2008b). Fragility-based assessment of typical mid-rise and low-rise RC buildings in Turkey, Eng. Struct. 30, 1360–1374.

Erdik, M., Doyuran, V., Akkas, P., and Gulkan, P. (1985) ‘‘Assessment of the earthquake hazard in Turkey and neighboring regions,’’ Tectonophysics 117, 295–344.

Evernden, J. F. and Thomson, J. M. (1985) ‘‘Predicting seismic intensities,’’ U.S. Geological Survey Professional Paper 1360, 151–202.

Hasancebi, N. and Ulusay, R. Bull Eng Geol Environ (2007) 66: 203. https://doi.org/10.1007/s10064-006-0063-0

Hashash, Y. M., Groholski, D. R., Phillips, C. A., Park, D., & Musgrove, M. (2012). DEEPSOIL 5.1. User Manual and Tutorial, 107.

Hassan, A. F., and Sözen, (1997) M. A. Seismic Vulnerability Assessment of Low-Rise Buildings in Regions with Infrequent Earthquakes. ACI Structural Journal.

Holzer, T. L., Toprak, S., and Bennett, M. J. (2002). Liquefaction potential index and seismic hazard mapping in the San Francisco Bay area, California. 7th National Conference on Earthquake Engineering, (June 2015), 1699–1706.

Idriss IM, Boulanger RW. Soil liquefaction during earthquakes. Earthquake Engineering Research Institute; 2008.

I.M. Idriss, R.W. Boulanger, SPT-based liquefaction triggering procedures, Report UCD/CGM-10/02, Department of Civil and Environmental Engineering, University of California, Davis, CA, 2010.

Ishihara, K., and Yoshimine, M. (1992). “Evaluation of settlements in sand deposits following liquefaction during earthquakes.” Soils Found. 32_1_, 173–188.

Istanbul Metropolitan Municipality Construction Directorate Geotechnical and Earthquake Investigation Department. Earthquake Master Plan for Istanbul, Istanbul, 2003; 1344.

Iwasaki, T., Tatsuoka, F., Tokida, K., and Yasuda, S. (1978). A Practical Method for Assessing Soil Liquefaction Potential Based on Case Studies at Various Sites in Japan. 2nd International Conference on Microzonation for Safer Construction Research and Application.

Iwasaki T., Arakawa, T. and Tokida, K. (1982), "Standard Penetration Test and Liquefaction Potential Evaluation", Proceedings, International Conference on Soil Dynamics and Earthquake Engineering, Southampton, Vol.2, pp. 925-941.

Kanıbir, A., Ulusay, R., & Aydan, Ö. (2006). Assessment of liquefaction and lateral spreading on the shore of Lake Sapanca during the Kocaeli (Turkey) earthquake. Engineering geology, 83(4), 307-331.

Karimzadeh, S., Askan, A., Erberik, M. A., and Yakut, A. (2018). Seismic damage assessment based on regional synthetic ground motion dataset : a case study for Erzincan,. Natural Hazards, 92(3), 1371–1397. https://doi.org/10.1007/s11069-018-3255-6

Liao, S. S., & Whitman, R. V. (1986). Overburden correction factors for SPT in sand. *Journal of geotechnical engineering*, *112*(3), 373-377.

NEHRP (1997). Recommended provisions for seismic regulations for new buildings and other structures. Report FEMA-303, Building Seismic Safety Council, Federal Emergency Management Agency, Washington DC.

Ohta, Y. and Goto, N. (1978), Empirical shear wave velocity equations in terms of characteristic soil indexes. Earthquake Engng. Struct. Dyn. 6: 167-187. doi:10.1002/eqe.4290060205

Sadigh, K., Chang, C.-Y., Egan, J. A., Makdisi, F., and Youngs, R. R. [1997] ''Attenuation relationships for shallow crustal earthquakes based on

California based on California strong motion data,'' Seismological Research Letters 68(1), 180–189.

Schnabel, P.B., Lysmer, J. and Seed, H. B. (1972), "SHAKE: A Computer Program for Earthquake Response Analysis of Horizontally Layered Sites", Earthquake Engineering Research Center, University of California, Berkeley, Berkeley, CA. Report No. EERC 72-12.

Schnabel, P.B. (1973). 'Effects of Local Geology and Distance from Source on Earthquake Ground Motion', Ph.D. Thesis, University of California, Berkeley, California.

Shamoto, Y., Zhang, J. M., and Tokimatsu, K. (1998). "Methods for evaluating residual post-liquefaction ground settlement and horizontal displacement." Soils Found. 2_2_, 69–83.

Seed, H. B. and Idriss, I. M. (1970), "Soil Moduli and Damping Factors for Dynamic Response Analyses", Report No. EERC 70-10, Earthquake Engineering Research Center, University of California, Berkeley, Berkeley, CA.

Seed, H. B. and Idriss, I. M. (1971), "Simplified Procedure for Evaluating Soil Liquefaction Potential", Journal of the Soil Mechanics and Foundations Division, ASCE, Vol. 97, No SM9, Proc. Paper 8371, September 1971, pp. 1249-1273.

Seed, H. B., Idriss, I.M and Arango, I. (1983), "Evaluation of Liquefaction Potential Using Field Performance Data and Cyclic Mobility Evaluation for Level Ground During Earthquakes ", Journal of Geotechnical Engineering, ASCE, Vol.109, No.3, pp. 458-482.

Seed, H. B., Wong, R. T., Idriss, I. M., and Tokimatsu, K. (1986). Moduli and Damping Factors for Dynamic Analyses of Cohesionless Soils. Journal of Geotechnical Engineering, 112(11), 1016–1032.

Spss, I. B. M. (2016). Statistics for Windows, Version 24. 0 [Computer Software]. Armonk, NY: IBM Corp.

Strasser, F. O., Bommer, J. J., Şeşetyan, K., Erdik, M., Çağnan, Z., Irizarry, J., Goula, X., Lucantoni, A., Sabetta, F., Bal, I. E., Crowley, H. and Lindholm, C. (2008). A Comparative Study of European Earthquake Loss Estimation Tools for a Scenario in Istanbul A Comparative Study of European Earthquake Loss Estimation Tools for a Scenario in Istanbul. 2469(May). https://doi.org/10.1080/13632460802014188

Sykora D.W. and Stokoe K.H. II. (1983). Correlations of in situ measurements in sands with shear wave velocity. The University of Texas at Austin.

Tokimatsu, K. and Seed, H. B. (1984). "Simplified procedures of the evaluation of settlements in clean sands." Rep. No. UCB/GT-84/16, Univ. of California, Berkeley, Calif.

Wetcher-Hendricks, D. (2011). Analyzing quantitative data: An introduction for social researchers. John Wiley & Sons.

Wu, J. and Seed, R. B. (2004). "Estimating of liquefaction-induced ground settlement _case studies_." Proc., 5th Int. Conf. on Case Histories in Geotechnical Engineering, Paper 3.09, New York.

Youd, T. L., et al. (2001). "Liquefaction resistance of soils: Summary report from the 1996 NCEER and 1998 NCEER/NSF workshops on evaluation of liquefaction resistance of soils." J. Geotech. Geoenviron. Eng., 127(10), 817–833.

Toprak, S., and Holzer, T. L. (2003). Liquefaction Potential Index : Field Assessment. 129(April), 315–322.

Toprak, S., Holzer, T. L., Bennett, M. J., and Tinsley, J. C. (1999). CPT-and SPT-based probabilistic assessment of liquefaction potential. 7th US–Japan Workshop on Earthquake Resistant Design of Lifeline Facilities and Countermeasures against Liquefaction, (August).

Ugurhan, B., Askan, A., and Erberik, M. A. (2011). A Methodology for Seismic Loss Estimation in Urban Regions Based on Ground-Motion Simulations. 101(2), 710–725. https://doi.org/10.1785/0120100159

Yakut, A., Ozcebe, G., and Yucemen, M. S. (2006). Seismic vulnerability assessment using regional empirical data. (January), 1187–1202. https://doi.org/10.1002/eqe.572

Yilmaz, Z. (2004). GIS-Based Structural Performance Assessment of Sakarya City After 1999 Kocaeli-Turkey Earthquake from Geotechnical and Earthquake Engineering Point of View (Master's thesis, Middle East Technical University).

Yilmaz, Z., and Cetin, K. O. (2003). GIS-Based Seismic Soil Liquefaction Assessment for Sakarya City after 1999 Kocaeli-Turkey Earthquake. 1, 7–9.

Youd, T. L., and Idriss, I. M. (1997) ''Summary report.'' Proc., NCEER Workshop on Evaluation of Liquefaction Resistance of Soils, Tech. Rep. NCEER-97-0022, National Center for Earthquake Engineering Research, Buffalo, N.Y.

Yucemen, M. S., Ozcebe, G., and Pay, A. C. (2004). Prediction of potential damage due to severe earthquakes. 26, 349–366. https://doi.org/10.1016/j.strusafe.2003.09.002

APPENDICES

A. Adapazarı Database Borehole Results

North Coordinate	East Coordinate	borehole nr	LSI	Settlement (in cms)
4510460	532816	54_222_sk1	2.01221	8.03666
4510586	533557	54_222_sk2	1.23925	4.67661
4511110	533760	54_222_sk3	1.48655	6.11362
4510560	534750	54_222_sk4	0.41953	4.82686
4511130	534850	54_222_sk5	0.00000	0.00000
4510172	533281	54_222_sk6	0.00000	0.00000
4510810	533510	54_222_sk7	1.70223	9.02636
4518615	536041	54_226_sk2	0.20245	0.59637
4518347	536011	54_226_sk4	0.00000	0.00000
4517897	536071	54_226_sk5	0.00000	0.00000
4517700	535828	54_226_sk6	0.00000	0.00000
4517525	536048	54_226_sk7	0.00000	0.00000
4517298	536405	54_226_sk8	3.31071	10.82428
4516769	536228	54_226_sk9	0.00000	0.00000
4506414	530583	54_229_sk10	0.29104	3.07029
4506209	530302	54_229_sk11	0.00000	0.00000
4509672	529883	54_229_sk12	0.00000	0.00000
4508972	529783	54_229_sk13	0.00000	0.00000
4508396	529774	54_229_sk14	0.00000	0.00000
4507679	529543	54_229_sk15	0.00000	0.00000
4507192	529685	54_229_sk16	0.00000	0.00000
4506692	529776	54_229_sk17	0.00000	0.00000
4506205	529882	54_229_sk18	0.01483	1.57957
4509880	528896	54_229_sk19	0.00000	0.00000
4508998	528847	54_229_sk20	0.44701	1.59225
4507602	529129	54_229_sk21	0.00000	0.00000
4507200	529083	54_229_sk22	0.00000	0.00000
4506606	529571	54_229_sk23	0.00000	0.00000
4509050	528349	54_229_sk24	1.47995	6.25217

North Coordinate	East Coordinate	borehole nr	LSI	Settlement (in cms)
4507534	528354	54_229_sk25	0.00000	0.00000
4507188	528172	54_229_sk26	0.00000	0.00000
4506550	528158	54_229_sk27	0.00000	0.00000
4510816	530058	54_229_sk28	0.00000	0.00000
4510221	529937	54_229_sk29	0.00000	0.00000
4510847	530771	54_229_sk3	0.00000	0.00000
4509426	528836	54_229_sk30	0.87388	2.51412
4508605	528761	54_229_sk31	0.00000	0.00000
4508528	528092	54_229_sk32	0.00000	0.00000
4506454	528838	54_229_sk33	0.00000	0.00000
4507617	529963	54_229_sk34	0.00000	0.00000
4508215	530236	54_229_sk35	0.00000	0.00000
4509134	530507	54_229_sk36	2.01098	18.28370
4509413	530483	54_229_sk37	0.00000	0.00000
4508726	530068	54_229_sk38	3.85899	16.33752
4510295	530515	54_229_sk4	0.46471	4.03259
4509494	530734	54_229_sk5	0.92483	8.36574
4508982	530549	54_229_sk6	1.03505	8.90167
4508300	530584	54_229_sk7	3.42708	11.46027
4507747	530569	54_229_sk8	0.05560	1.17134
4507235	530548	54_229_sk9	0.58660	3.70034
4514164	533247	54_230_sk1	3.09381	9.02081
4515383	534108	54_230_sk10	3.37109	9.95840
4515631	533840	54_230_sk11	1.84926	6.05896
4515648	534227	54_230_sk12	4.46677	18.28588
4516010	534163	54_230_sk13	3.86774	20.00602
4516540	534160	54_230_sk14	1.35000	5.72382
4516980	534260	54_230_sk15	0.64498	2.20165
4516860	534830	54_230_sk16	3.67655	13.68139
4515900	535220	54_230_sk17	4.50609	17.66090
4516817	535562	54_230_sk18	1.48697	4.75970
4517910	534440	54_230_sk19	5.09029	20.29665
4513852	532902	54_230_sk2	0.00000	0.00000
4517870	533910	54_230_sk20	1.04893	4.07729

North Coordinate	East Coordinate	borehole nr	LSI	Settlement (in cms)
4517860	535250	54_230_sk21	7.46422	24.85310
4518800	534910	54_230_sk22	7.62386	49.12550
4517590	533420	54_230_sk23	5.17513	20.41506
4517620	532720	54_230_sk24	8.30832	30.62863
4516980	532820	54_230_sk25	7.19980	28.59338
4516990	533350	54_230_sk26	1.88416	6.69910
4516310	533050	54_230_sk27	2.23845	8.41066
4516540	533480	54_230_sk28	0.00000	0.00000
4516330	533440	54_230_sk29	4.06400	18.42597
4514545	532248	54_230_sk3	1.61281	7.40828
4517180	532110	54_230_sk30	1.88616	4.64018
4515959	533500	54_230_sk31	2.88052	8.95132
4515127	534636	54_230_sk32	2.01300	2.20000
4516510	533850	54_230_sk33	0.00000	0.00000
4516331	534493	54_230_sk34	5.79654	32.33487
4514854	535263	54_230_sk35	1.50412	4.38827
4517410	533840	54_230_sk36	3.45432	12.37000
4519040	534253	54_230_sk37	1.48312	5.38642
4514714	532749	54_230_sk4	1.71182	8.55011
4517290	531640	54_230_sk40	1.65766	4.47648
4516220	532150	54_230_sk41	0.00000	0.00000
4517990	533200	54_230_sk43	1.37946	5.30631
4518510	533650	54_230_sk45	0.00000	0.58204
4516760	534980	54_230_sk46	2.57976	6.81811
4515180	533164	54_230_sk5	1.54251	7.59331
4515020	534860	54_230_sk51	0.00000	0.00000
4518170	534310	54_230_sk54	2.68607	6.30028
4515574	533262	54_230_sk6	0.00000	0.00000
4516040	533870	54_230_sk62	1.29297	8.25695
4515920	533700	54_230_sk64	0.57969	1.72259
4513820	532380	54_230_sk65	8.78037	40.97772
4514220	532510	54_230_sk66	0.00000	0.00000
4513970	531980	54_230_sk67	6.90515	78.48512
4515180	533802	54_230_sk7	2.94359	9.17062

North Coordinate	East Coordinate	borehole nr	LSI	Settlement (in cms)
4513490	531780	54_230_sk71	0.01634	2.43142
4514250	532110	54_230_sk72	2.29850	8.35185
4515260	532610	54_230_sk73	0.00000	0.00000
4516000	532590	54_230_sk76	1.98500	9.83173
4516760	531770	54_230_sk77	0.00000	0.00000
4517300	531500	54_230_sk78	1.15905	4.38612
4515111	534130	54_230_sk8	2.82477	9.41430
4516190	532640	54_230_sk88	3.49476	15.76731
4516460	534320	54_230_sk89	6.95812	106.22362
4515320	534503	54_230_sk9	0.00366	0.34066
4515600	534280	54_230_sk90	0.00000	0.00000
4517740	533570	54_230_sk91	1.05000	5.35312
4514690	533360	54_230_sk92	2.80103	16.91840
4516230	533480	54_230_sk93	2.88564	15.71785
4514790	532710	54_230_sk94	2.10471	11.04471
4512100	534100	54_232_sk10	1.57605	4.06392
4512490	534010	54_232_sk11	0.00000	0.00000
4512330	533840	54_232_sk12	0.01694	1.60615
4512870	533990	54_232_sk13	0.00000	0.00000
4512700	534280	54_232_sk14	0.00000	0.00000
4512340	534570	54_232_sk15	1.59305	5.54363
4512940	534670	54_232_sk16	1.85041	20.33997
4513310	534670	54_232_sk17	1.82792	7.83101
4512450	532860	54_232_sk18	0.00000	0.00000
4512970	535520	54_232_sk19	1.08927	4.15771
4512230	533090	54_232_sk2	0.29343	0.71042
4512890	535890	54_232_sk20	2.26451	6.96918
4513150	535790	54_232_sk21	0.00000	0.00000
4513510	534760	54_232_sk22	0.00000	0.00000
4513390	535760	54_232_sk23	2.43323	19.65713
4513030	535030	54_232_sk24	0.00000	0.00000
4513850	535490	54_232_sk25	0.67349	3.23678
4512580	534960	54_232_sk26	3.03243	27.33841
4513490	535110	54_232_sk27	0.44400	2.82754

North Coordinate	East Coordinate	borehole nr	LSI	Settlement (in cms)
4513590	534470	54_232_sk28	7.17284	39.15469
4513720	535190	54_232_sk29	0.15839	2.14741
4512430	533160	54_232_sk3	0.16938	0.25000
4513830	534510	54_232_sk30	1.99311	5.84369
4514160	534690	54_232_sk32	0.95049	5.36295
4514060	535140	54_232_sk33	2.96326	26.76483
4513840	534790	54_232_sk34	2.58174	6.13509
4515120	535280	54_232_sk35	0.00000	0.49445
4513860	534940	54_232_sk36	1.26462	3.09314
4515060	535040	54_232_sk37	0.27589	1.58763
4514360	534500	54_232_sk38	0.00000	0.00000
4514460	534700	54_232_sk39	0.65790	2.24189
4512510	533260	54_232_sk4	0.00000	0.00000
4514060	534870	54_232_sk40	0.49033	2.89355
4514170	534360	54_232_sk41	6.48432	36.61514
4514480	534400	54_232_sk42	8.17351	54.55459
4514740	534680	54_232_sk43	4.09980	16.08008
4514220	534120	54_232_sk44	8.74635	47.86036
4514730	534350	54_232_sk45	7.43626	52.08664
4514440	534120	54_232_sk46	9.20997	47.67722
4513900	534140	54_232_sk47	3.69187	22.43185
4513880	533910	54_232_sk48	0.79007	2.49252
4514660	533940	54_232_sk49	1.07032	2.54884
4512210	533480	54_232_sk5	0.33772	0.99921
4514720	533500	54_232_sk50	2.27208	10.37640
4513360	533810	54_232_sk52	0.00000	0.00000
4513400	533370	54_232_sk53	0.00000	0.00000
4513060	533450	54_232_sk54	0.00000	0.00000
4513620	533830	54_232_sk55	1.50667	4.36202
4513620	533570	54_232_sk56	1.56353	3.94813
4513840	533440	54_232_sk57	1.91920	4.73076
4513850	533690	54_232_sk58	1.57987	5.30445
4513800	533280	54_232_sk59	1.50879	5.41879
4512640	533320	54_232_sk6	0.00000	0.00000

North Coordinate	East Coordinate	borehole nr	LSI	Settlement (in cms)
4514020	533510	54_232_sk60	0.00000	0.00000
4514240	533610	54_232_sk61	4.80018	49.04581
4514250	533840	54_232_sk62	3.91242	39.56650
4514470	533710	54_232_sk63	4.39461	47.31358
4514230	534610	54_232_sk64	0.93995	5.37143
4512060	534980	54_232_sk65	1.70685	5.13662
4512420	532680	54_232_sk66	0.00000	0.00000
4512170	532710	54_232_sk67	0.00000	0.00000
4514890	534230	54_232_sk68	7.86312	54.59018
4512680	533460	54_232_sk69	0.00000	0.00000
4512320	533630	54_232_sk7	1.03405	3.68956
4512360	533590	54_232_sk8	0.00000	0.00000
4511970	533740	54_232_sk9	0.77718	5.02690
4509071	534840	54_244_sk1	1.95364	12.18262
4507380	531689	54_244_sk10	2.01235	11.95654
4508640	534449	54_244_sk2	2.21113	9.33065
4508277	533858	54_244_sk3	0.81734	9.25641
4508543	533388	54_244_sk4	0.54421	4.36199
4508892	532955	54_244_sk5	1.03159	6.33366
4508339	532129	54_244_sk6	5.64134	15.53565
4508106	531594	54_244_sk7	3.57752	9.72379
4507660	531489	54_244_sk8	4.14988	13.47283
4507170	531430	54_244_sk9	4.13824	14.43981
4515083	532465	54_sau_scm210	1.81455	9.09535
4516105	533764	54_sau_scm224	0.00000	1.06580
4516260	533319	54_sau_scm242	3.33399	10.05011
4514730	533496	54_sau_sdl464	1.19505	5.84321
4516179	534731	54_sau_sdl483	0.00000	0.00000
4511748	534666	54_sau_ser531	0.00000	0.00000
4511872	534928	54_sau_ser533	0.01571	0.79663
4512113	534173	54_sau_ser536	1.66507	3.75374
4513324	534448	54_sau_ser540	0.58963	2.09110
4511590	534067	54_sau_ser543	0.07451	0.96902
4513694	534836	54_sau_ser548	0.83879	2.11897

North Coordinate	East Coordinate	borehole nr	LSI	Settlement (in cms)
4512960	533784	54_sau_ser593	0.00000	0.00000
4511230	533420	54_sau_shn08	0.14357	2.69069
4510076	532647	54_sau_shn09	0.32062	5.16081
4510890	532760	54_sau_shn10	2.12779	7.48587
4510411	533901	54_sau_shn11	0.00000	0.00000
4511210	533980	54_sau_shn12	0.00010	0.58360
4510501	533419	54_sau_shn13	0.00000	0.00000
4514676	533800	54_sau_sho485	0.11416	1.37583
4516652	533622	54_sau_sis326	0.81331	5.41142
4516705	533107	54_sau_sis572	1.69972	5.69342
4516898	534387	54_sau_sko409	0.00000	0.00000
4513742	535458	54_sau_skp506	0.00000	0.62943
4515103	532498	54_sau_smp416	0.00000	0.00000
4514572	532838	54_sau_smp428	0.00927	2.08169
4514657	532077	54_sau_smp438	0.00000	0.00000
4514682	532635	54_sau_smp461	2.46299	11.37824
4515890	532330	54_sau_smp566	0.00000	0.00000
4516332	533982	54_sau_sor265	0.25298	2.32844
4516612	534342	54_sau_sor415	0.00000	0.00000
4517155	533067	54_sau_soz363	0.01252	1.75563
4515661	534286	54_sau_soz383	1.42637	3.47226
4516986	533823	54_sau_ssa392	0.73401	5.90229
4517011	532109	54_sau_ssk341	0.35923	2.20487
4517114	532675	54_sau_ssk342	0.90500	1.37475
4517258	532841	54_sau_ssk349	0.45250	0.73469
4516081	532671	54_sau_ssk360	3.46286	13.01125
4517198	531661	54_sau_ssk584	1.96513	8.55123
4515582	533257	54_sau_ssm177	0.00000	0.73690
4515909	533039	54_sau_ssm186	0.03308	1.21371
4515587	533840	54_sau_ssm189	0.14016	0.81598
4517830	533760	54_sau_ste403	0.00000	0.22596
4518577	534205	54_sau_ste406	0.27127	1.31467
4515784	534254	54_sau_stı028	2.80301	13.29036
4518243	534987	54_sau_stz620	0.00185	0.18866

North Coordinate	East Coordinate	borehole nr	LSI	Settlement (in cms)
4516776	534861	54_sau_sya301	0.00000	0.00000
4517015	535543	54_sau_sya304	0.04909	0.56481
4516822	535448	54_sau_sya307	2.49315	9.20977
4515965	534786	54_sau_sya308	2.36794	10.25465
4516008	535203	54_sau_sya311	4.06094	16.36590
4515365	534148	54_sau_syc122	0.27324	1.46058
4515169	533935	54_sau_syc123	0.00000	0.14261
4515191	533503	54_sau_syd158	0.84528	3.93611
4515117	533114	54_sau_syd160	0.51625	2.47845
4515034	535010	54_sau_syg079	0.00000	0.15556
4515765	534620	54_sau_syg100	2.71298	6.46866
4515222	534601	54_sau_syg62	1.90574	4.52621
4515800	535014	54_sau_syg87	3.65150	12.11025
4512450	535212	54_sau_sym507	1.55984	9.28983
4513304	535081	54_sau_sym513	0.01442	1.73039
4512641	535583	54_sau_sym607	0.69560	2.31330
4513151	535445	54_sau_sym611	0.75551	4.77480

B. Düzce Database Borehole Results

East Coord.	North Coord.	Hole No	LSI	S (in cms)	PGA	SA T= 0.3	SA T= 0.4	SA T= 0.5	SA T= 0.6
598237	4523431	1	0.80000	0.59	0.60874	2.85715	1.54120	1.02912	0.85544
598063	4523477	2	1.10000	0.91	0.50078	2.40194	1.53160	0.87900	0.68507
598022	4523436	3	3.50621	7.94	0.53931	2.56349	1.60150	0.95509	0.72621
597807	4523456	4	0.78135	0.69	0.53263	2.46072	1.40218	0.97404	0.82121
598118	4523724	5	0.60251	0.57	0.72366	3.47337	2.06469	0.92522	0.64247
598227	4523854	6	1.93052	6.11	0.43129	2.04676	1.25434	0.79612	0.69235
598065	4523806	7	3.12062	12.45	0.69326	3.38272	1.97568	1.00143	0.71055
598303	4523338	8	2.40000	5.83	0.57809	2.79506	1.77694	0.90125	0.65656
597679	4523366	9	4.45420	15.22	0.38119	1.73581	1.11425	0.81318	0.74305
597929	4523747	10	2.97916	12.06	0.40766	1.83171	1.10911	0.83026	0.78301

East Coord.	North Coord.	Hole No	LSI	S (in cms)	PGA	SA T= 0.3	SA T= 0.4	SA T= 0.5	SA T= 0.6
597880	4523868	11	1.32950	0.71	0.65595	3.16082	1.88806	0.85058	0.61974
597794	4523828	12	1.10000	0.71	0.60853	2.93330	1.83710	0.89261	0.64536
597758	4523887	13	1.22100	2.40	0.76724	3.71465	2.22508	1.04156	0.68653
597658	4523949	14	3.41515	8.01	0.71581	3.48104	2.01436	0.93552	0.66339
597608	4523832	15	3.35770	16.30	0.67402	3.24585	1.94020	0.95207	0.67866
597553	4523587	16	1.19605	1.18	0.63139	3.04996	1.87553	0.87342	0.63103
597954	4523543	17	2.42500	12.70	0.61106	2.92884	1.81851	0.91419	0.66341
597941	4523647	18	2.38261	13.91	0.54965	2.63395	1.64291	0.83772	0.64084
597197	4523909	19	1.68262	3.85	0.60360	2.84997	1.48400	1.02214	0.91328
597758	4523652	19	1.68262	3.85	0.60360	2.84997	1.48400	1.02214	0.91328
597997	4523300	20	6.40969	17.81	0.44210	2.01609	1.21440	0.84036	0.75112
598242	4523623	21	3.22800	7.18	0.45787	2.08121	1.20344	0.91145	0.84536
598149	4523218	22	2.33196	3.88	0.56431	2.69679	1.25805	0.81866	0.89973
598242	4523144	23	3.06143	7.01	0.43789	1.95249	0.95292	0.51836	0.80626
598425	4523764	24	3.55375	15.77	0.55684	2.57295	1.30097	0.95160	0.96712
598411	4523942	25	2.32841	3.78	0.50866	2.42884	1.54308	0.80330	0.63127
597533	4523908	26	4.72500	13.50	0.67365	3.26802	1.94319	0.97902	0.69717
597510	4523823	27	2.77354	8.80	0.50887	2.38879	1.43463	0.92637	0.75781
597429	4523420	28	1.72500	1.93	0.67435	3.24006	1.96720	0.90342	0.63944
598429	4523170	29	0.86376	0.36	0.59572	2.89052	1.77816	0.83299	0.61898
597425	4523842	30	3.51000	7.50	0.52440	2.49610	1.53605	0.91111	0.71704
597378	4523727	31	4.37386	23.67	0.39732	1.81707	0.90441	0.64316	0.83779
598616	4523941	33	4.48000	17.84	0.45044	2.06586	1.25912	0.88471	0.77213
597185	4523932	34	1.74948	2.31	0.48401	2.23711	1.33559	0.83575	0.71136
597153	4523906	36	6.14910	33.21	0.52553	2.39914	1.39298	0.91901	0.77500
597133	4523882	37	4.67059	23.33	0.59239	2.86096	1.79598	0.85668	0.62789
597208	4523827	38	5.16775	24.31	0.44772	2.04910	1.27204	0.87751	0.75782
597164	4523743	39	0.00009	1.65	0.52850	2.58105	1.58502	0.73639	0.58295
597116	4523714	40	2.23581	7.45	0.54674	2.68637	1.63158	0.75162	0.58959
597068	4523783	41	5.83254	21.83	0.57965	2.83672	1.72746	0.79605	0.60484

East Coord.	North Coord.	Hole No	LSI	S (in cms)	PGA	SA T= 0.3	SA T= 0.4	SA T= 0.5	SA T= 0.6
597066	4523962	42	0.00000	0.00	0.61248	2.98411	1.83113	0.84658	0.62045
596957	4523897	43	0.00000	0.00	0.61248	2.98411	1.83113	0.84658	0.62045
596912	4523646	44	7.25256	38.61	0.42054	1.93723	0.98100	0.70856	0.86491
597465	4523605	45	2.52937	14.27	0.53810	2.55650	1.61487	0.92415	0.69923
597385	4523646	46	4.98602	31.69	0.60276	2.84235	1.55924	1.01493	0.83228
597276	4523646	48	2.00988	6.45	0.55633	2.65600	1.21093	0.77381	0.91658
597169	4523461	49	4.79928	15.74	0.48186	2.18882	1.22857	0.91503	0.84545
597052	4523452	50	4.61219	14.53	0.52506	2.53698	1.60299	0.75599	0.59200
596858	4523848	51	4.12415	11.03	0.55903	2.70473	1.66020	0.78378	0.60491
596751	4523511	52	5.48404	21.76	0.68169	3.30460	1.93980	0.91032	0.65480
596672	4523614	53	6.46248	21.93	0.49734	2.28589	1.33972	0.86480	0.74013
596438	4523624	54	2.60040	6.65	0.44361	2.10287	1.28440	0.79219	0.68136
596307	4523620	55	7.06938	24.53	0.41760	1.97178	1.23438	0.79899	0.69523
596362	4523516	56	8.10169	30.86	0.41459	1.85286	1.13596	0.85385	0.79286
596281	4523533	57	1.64510	3.14	0.43534	2.01939	1.24139	0.80778	0.70528
596204	4523522	58	5.65537	20.59	0.63227	3.07860	1.80996	0.78336	0.58960
596213	4523607	59	4.42629	8.96	0.55736	2.75010	1.67492	0.77049	0.59640
595998	4523543	60	2.94748	10.95	0.61158	2.88616	1.53267	1.00844	0.85114
595998	4523440	61	3.42049	6.79	0.47955	2.21313	1.28778	0.85169	0.74131
595926	4523369	62	7.73893	33.16	0.63975	3.12427	1.65643	1.02132	0.86803
595765	4523631	63	2.81636	16.22	0.54036	2.67227	1.61100	0.74065	0.58493
595796	4523882	64	4.78487	14.20	0.58663	2.82747	1.80525	0.87727	0.63610
595525	4523731	65	5.31667	14.10	0.47268	2.18227	1.30939	0.82934	0.71176
595484	4523384	66	2.85547	13.11	0.56399	2.77600	1.68499	0.77238	0.59633
595331	4523884	67	3.84015	17.12	0.56231	2.77379	1.65572	0.75431	0.59081
595311	4523618	68	3.81419	10.99	0.51474	2.50618	1.53145	0.71542	0.57429
595229	4523341	69	4.65681	18.81	0.49277	2.34780	1.49112	0.77896	0.62186
596973	4523240	70	5.72363	12.44	0.53595	2.61212	1.60573	0.75068	0.59085
597054	4522898	71	6.68093	22.91	0.58613	2.83764	1.77629	0.84020	0.62083
597238	4523066	76	4.72142	13.22	0.51368	2.43592	1.54609	0.82117	0.64217

East Coord.	North Coord.	Hole No	LSI	S (in cms)	PGA	SA T= 0.3	SA T= 0.4	SA T= 0.5	SA T= 0.6
597597	4522374	77	2.54100	4.62	0.61127	2.99232	1.83385	0.84809	0.62163
597471	4522824	78	3.52702	20.81	0.65990	3.19054	1.98865	1.06189	0.72698
597516	4523128	79	6.66305	27.85	0.54845	2.52474	1.32759	0.96267	0.89927
597673	4523313	80	1.47657	2.00	0.53041	2.43234	1.20862	0.83589	0.85499
597690	4523186	81	0.00000	0.19	0.50844	2.45073	1.53854	0.72829	0.58004
597656	4522928	82	8.17779	47.73	0.61693	2.99374	1.80321	1.08895	1.15479
597693	4522706	83	0.00000	0.00	0.54102	2.53576	1.56479	1.12860	0.87257
597861	4523216	84	7.77269	42.83	0.62117	2.93624	1.36615	0.88440	0.89542
597782	4523063	85	4.70798	18.20	0.54860	2.66320	1.66476	0.77716	0.59837
597961	4523098	86	5.79319	22.89	0.51857	2.39762	1.36182	0.94360	0.81059
597928	4522947	87	4.73275	12.51	0.55417	2.67959	1.64202	0.78954	0.61171
598109	4522320	88	3.30085	8.12	0.51245	2.49526	1.52528	0.71422	0.57406
598208	4522999	89	3.64168	13.39	0.24921	1.03087	0.54814	0.31740	0.57512
598259	4522922	90	3.54083	10.01	0.52192	2.51361	1.56104	0.74784	0.59241
598481	4522870	92	1.45629	4.76	0.38132	1.66223	0.87277	0.68703	0.82947
598569	4522627	93	4.25250	14.97	0.60368	2.94859	1.79103	0.81916	0.61085
598811	4522476	94	0.00000	0.00	0.60572	2.91062	1.81545	0.84904	0.62089
598627	4522945	94	0.00000	0.00	0.60572	2.91062	1.81545	0.84904	0.62089
598656	4523120	95	0.00000	0.00	0.60268	2.91729	1.79693	0.83196	0.61490
598626	4523389	96	3.70824	9.48	0.42886	2.00937	1.22672	0.81367	0.71764
598783	4523074	97	2.60927	3.22	0.47233	2.18208	1.30521	0.83926	0.72348
598904	4523241	99	0.73466	0.82	0.35790	1.56509	0.95127	0.67773	0.68244
598934	4523132	100	0.00000	0.00	0.64330	3.10548	1.92977	0.90004	0.63812
598987	4522981	101	0.00000	0.00	0.60948	2.92005	1.91461	0.98323	0.67917
599355	4523668	102	1.82400	1.98	0.55612	2.65647	1.59749	0.92623	0.72140
599119	4523358	103	0.00000	0.00	0.65060	3.10751	1.98541	0.96388	0.66298
599195	4523279	104	0.74076	3.61	0.53418	2.60716	1.53264	0.66147	0.53866
599424	4523573	106	1.70893	2.29	0.64922	3.11051	1.89013	0.85926	0.62152
599397	4523187	107	3.64363	8.47	0.60490	2.89010	1.76913	0.86725	0.64394
600124	4523233	110	2.58383	2.32	0.63777	3.07719	1.90880	0.89467	0.63765

East Coord.	North Coord.	Hole No	LSI	S (in cms)	PGA	SA T= 0.3	SA T= 0.4	SA T= 0.5	SA T= 0.6
600448	4523632	111	0.00000	0.00	0.64214	3.05656	1.95796	0.95262	0.65891
600605	4523318	112	0.05563	0.29	0.58040	2.78762	1.83961	0.96658	0.67831
600533	4522978	113	0.71775	0.42	0.51601	2.44226	1.60728	0.98272	0.72563
600641	4523488	114	3.54713	4.69	0.64348	3.08904	1.93617	0.93453	0.65661
600879	4522071	125	1.24259	2.92	0.53013	2.57501	1.57675	0.73478	0.58279
601446	4522165	126	0.78687	5.09	0.49688	2.39271	1.47180	0.69290	0.56396
597612	4524308	148	3.35149	10.52	0.59541	2.86505	1.81587	0.86726	0.62982
593927	4524591	149	1.61873	4.24	0.38577	1.81816	1.17145	0.74571	0.65691
595162	4524377	151	3.01582	6.02	0.57072	2.76539	1.66893	0.77550	0.60059
595407	4524500	152	1.03556	4.18	0.23420	0.96388	0.55920	0.41835	0.67274
595584	4524113	153	0.45409	1.45	0.55639	2.75712	1.64587	0.75207	0.59032
595988	4524488	155	1.59942	5.53	0.54538	2.68186	1.60942	0.74171	0.58631
595997	4524200	156	6.45798	21.21	0.61729	2.97285	1.80258	0.83182	0.61696
596302	4524403	158	3.16450	8.32	0.50639	2.43342	1.57583	0.86226	0.66035
596472	4524004	159	0.70104	0.22	0.56818	2.77991	1.69720	0.78240	0.60039
596680	4524321	160	0.56558	0.51	0.61093	2.95386	1.78112	0.81193	0.60825
596750	4524506	161	0.32366	0.90	0.51426	2.49921	1.52966	0.71430	0.57354
596888	4524167	162	0.00000	0.00	0.53907	2.64407	1.62209	0.75127	0.58940
596837	4524166	163	0.06124	0.02	0.54865	2.69801	1.64204	0.75625	0.59154
597123	4524164	164	0.00000	0.00	0.51894	2.52062	1.55718	0.72701	0.57873
596994	4524688	165	0.26907	1.12	0.51482	2.50865	1.52744	0.71141	0.57215
597189	4524299	166	0.14613	0.10	0.61424	2.97138	1.82235	0.84445	0.62036
597547	4524152	167	0.08234	0.02	0.60135	2.92655	1.76286	0.80266	0.60512
597637	4524053	168	0.08610	0.02	0.61395	2.95436	1.82163	0.84507	0.61959
597805	4524073	169	0.44293	0.99	0.59570	2.91251	1.71851	0.77467	0.59636
597915	4524176	170	0.00000	0.00	0.56779	2.73957	1.74387	0.84165	0.62385
597841	4524371	171	1.95194	5.62	0.55285	2.66463	1.62320	0.81896	0.63713
598184	4524134	172	0.00000	0.00	0.59308	2.85013	1.81478	0.87432	0.63303
598196	4524676	173	0.14401	2.32	0.51047	2.47978	1.51647	0.70974	0.57175
598386	4524438	174	0.84164	2.09	0.55357	2.70175	1.64215	0.76528	0.59778

East Coord.	North Coord.	Hole No	LSI	S (in cms)	PGA	SA T= 0.3	SA T= 0.4	SA T= 0.5	SA T= 0.6
598391	4525107	175	0.00000	0.00	0.53399	2.62173	1.60345	0.74086	0.58441
598425	4524144	176	0.16540	8.31	0.51717	2.52334	1.53801	0.71723	0.57508
598550	4524912	177	0.92091	0.39	0.53379	2.60243	1.60003	0.74852	0.58986
599234	4524341	179	0.92022	5.46	0.52629	2.55764	1.56516	0.73447	0.58409
599367	4524749	181	1.02979	5.80	0.52193	2.52516	1.55819	0.73880	0.58729
597805	4524829	182	0.17142	0.74	0.51384	2.50041	1.52773	0.71242	0.57251
596959	4522598	201	6.45045	35.70	0.49313	2.32163	1.45868	0.90610	0.72703
597158	4522850	202	3.73540	16.38	0.23038	0.88111	0.51723	0.42741	0.71908
597376	4522832	203	4.29460	15.78	0.83660	4.12353	2.23381	1.00877	0.70165
597617	4523075	204	3.68443	9.42	0.51133	2.41216	1.48219	0.85793	0.68821
597423	4523042	205	6.24458	26.63	0.63367	3.06156	1.82091	1.09502	0.79009
597045	4522996	207	6.42673	33.25	0.38308	1.71814	0.93187	0.74507	0.84606
597052	4523161	208	6.63056	28.38	0.61982	2.98704	1.82763	1.06866	0.75986
597265	4523228	209	5.95129	20.63	0.63729	3.05085	1.84975	0.85697	0.62594
597489	4523222	210	3.88472	14.47	0.48629	2.33233	1.45975	0.75979	0.61393
597038	4523475	211	6.03517	35.17	0.46032	2.05701	1.08641	0.85825	0.90638
597015	4523569	212	6.31373	28.82	0.58567	2.76440	1.63815	0.92149	0.71430
597311	4523607	213	6.66113	29.05	0.57700	2.74769	1.63888	0.85310	0.66352
597301	4523436	214	6.33643	24.35	0.51873	2.43991	1.52229	0.93985	0.73651
597471	4523436	215	6.50063	20.21	0.51159	2.51098	1.54770	0.77497	0.61488
597483	4523608	216	4.75943	18.88	0.33223	1.50166	0.85484	0.64983	0.80226
597669	4523416	217	6.36303	31.03	0.63995	3.06737	1.81674	0.95226	0.70100
597695	4523617	218	5.01013	19.80	0.65314	3.22298	1.86744	0.77786	0.58017
597463	4523765	219	5.31282	20.79	0.59357	2.83390	1.61661	0.93006	0.74122
597234	4523789	220	5.46689	23.57	0.51520	2.42538	1.48370	0.84879	0.68322
597002	4523752	221	6.48184	30.97	0.63808	3.00122	1.76824	0.95976	0.71576
596947	4523943	222	6.64067	27.80	0.70643	3.44997	1.92579	0.99759	0.72977
597269	4523990	223	6.23875	23.24	0.51421	2.46342	1.52233	0.82814	0.65886
597520	4523984	224	4.75124	16.76	0.63970	3.02235	1.79172	0.85456	0.63886
597733	4523787	225	5.69200	23.77	0.53974	2.54828	1.55651	0.85114	0.67111

East Coord.	North Coord.	Hole No	LSI	S (in cms)	PGA	SA T= 0.3	SA T= 0.4	SA T= 0.5	SA T= 0.6
598169	4524020	227	5.72370	29.74	0.67616	3.24456	1.98771	1.00347	0.69592
598078	4523784	228	4.57118	30.71	0.71366	3.49413	1.94805	1.09686	0.80415
597910	4523755	229	5.89885	32.86	0.56248	2.68879	1.70366	0.94030	0.69308
597985	4523610	230	6.66943	23.72	0.50592	2.37209	1.44127	0.87409	0.71090
598025	4523379	232	6.27871	30.55	0.55729	2.60151	1.50719	1.08479	0.89024
598194	4523311	233	5.29734	30.05	0.47992	2.20299	1.29663	0.91564	0.79944
598308	4523145	234	6.59149	32.96	0.59353	2.79412	1.69218	0.97325	0.72985
598614	4523189	235	3.17880	7.15	0.60841	2.92089	1.75713	0.89381	0.66875
598317	4523481	236	4.39509	21.23	0.57997	2.72769	1.65914	0.96282	0.72804
598455	4523696	237	2.29736	18.04	0.24104	0.97815	0.61689	0.38986	0.66136
598610	4523797	238	4.84037	19.55	0.49704	2.38067	1.46210	0.79700	0.64535
598372	4524046	240	4.61060	11.25	0.43168	1.99986	1.26642	0.83735	0.71682
595291	4523174	241	0.00000	0.00	0.50265	2.39307	1.47376	0.85467	0.68825
595832	4523249	242	0.89205	0.45	0.62468	2.94185	1.75487	0.91684	0.68605
595983	4523544	243	6.22687	23.15	0.50163	2.42827	1.49332	0.83174	0.66780
595737	4523488	244	0.00000	0.00	0.46077	2.22020	1.39679	0.78514	0.64416
595417	4523451	245	6.81498	27.90	0.60048	2.82089	1.66917	0.93906	0.72044
595292	4523491	246	3.98980	22.66	0.54823	2.59657	1.55863	0.84520	0.67284
595469	4523738	247	5.54949	17.87	0.49083	2.27964	1.30621	0.89552	0.78405
595708	4523705	248	5.57243	18.66	0.48796	2.36731	1.46904	0.83298	0.67073
595654	4523999	249	0.00000	0.00	0.41309	1.89757	1.09101	0.80511	0.80505
595999	4524241	250	4.93137	23.40	0.56869	2.71239	1.56728	0.89087	0.71433